Detection of polysaccharides on a bacterial cell surface using Atomic Force Microscopy

by

Bhupinder S. Arora

A Thesis

submitted to the faculty of

WORCESTER POLYTECHNIC INSTITUTE

in partial fulfillment of the requirements for the

Degree of Masters of Science

in

Chemical Engineering

by

August, 2003

Approved:

Terri A. Camesano, Ph.D., Major Advisor
Assistant Professor of Chemical Engineering
Worcester Polytechnic Institute

Approved:

Ravindra Datta, Ph.D., H.O.D
Professor of Chemical Engineering
Worcester Polytechnic Institute

Contents

Acknowledgement

I wish to thank my advisor Prof. Terri Camesano for her invaluable guidance throughout this work. I highly appreciate her believing in me and giving me a chance to work on this project. I would also like to thank all the faculty members of the department of chemical engineering at WPI for providing me with the opportunity to pursue my masters in this institution. I am thankful to the department for funding me throughout the period of my education in this department.

I would like to extend my thanks to Nehal for training me on using the atomic force microscope and for helping me initiate my research. I would also like to thank Ray and Nehal for all the discussions that made my progress in the project, faster.

Finally I want to thank my parents and sister for their understanding, patience and moral support which kept me kicking through my thesis.

Detection of polysaccharides on a bacterial cell surface using Atomic Force Microscopy

1.0 Introduction

The polysaccharides present on a bacterial cell surface play a major role in deciding the adhesive nature of the cell towards surfaces such as soil. The adhesive nature of the bacterial cells has applications spanning a number of areas of research, such as in biomedical engineering, environmental science, etc. (Fletcher and Williams, 1996, Fletcher, DeFlaun, et al., 1999, Zehnder, Simoni, et al., 1998, Ouwehand, Salminen, et al., 2002). Bacterial adhesion may result in biofilm formation on teeth (in the form of dental plaque), artificial joints or other biomaterials such as endotracheal tubes (Triandafillu, Harms, et al., 2003), soil, and glass (Poelstra, Anthony, et al., 2000, Poortinga, Busscher et al., 2001, Sorongon, Burchard et al., 1991); in fouling of water-supply systems and bioreactors; in failure of contact lenses; in subsurface soil remediation; in microbial dissolution of minerals; in cell to cell transfer of genetic material and in microbial uptake of metals. In nature bacteria are mostly found as adhered to surfaces rather than unattached (Tombs and Harding, 1997).

Most of the research in the field of bacterial adhesion concentrates on reducing bacterial adhesion by making natural and engineered systems free of biofouling, where bacteria tend to attach and reduce the efficiency of these systems such as heat exchangers and bioreactors or surfaces which are hydrophobic (Holmberg and Harris,

1998). Some of the studies use techniques like confocal laser microscopy (CLM), scanning electron microscopy (SEM), transmission electron microscopy (TEM) and Fourier transform infrared spectroscopy (FTIR) to deduce the cause of these bacterial adhesions and biofilms formations by studying the structure of the biofilms during their genesis (Mittelman, 1998).

Previous attempts were made to explain bacterial adhesion in terms of the Derjaguin, Landau, Verwey and Overbeek (DLVO) theory of colloidal stability, considering the bacterial cell to be a colloid. Thus bacterial adhesion was modeled as if the process was controlled by electrostatic and van der Waals interactions (Israelachvili, 1992). However the polysaccharides present on the cell surface make the cells behave differently than model colloids, especially under conditions of low ionic strength where the polysaccharides are fully extended from the cell surface (Abu-Lail and Camesano, 2002). The polysaccharides present on the cell surface contribute large steric repulsion while the cell moves towards the surface such that the actual cell body never gets as close to the surface of the substratum as the primary minima calculated by DLVO theory. These polysaccharides may increase the overall attraction towards the substratum due to covalent bonding of the groups present on the polysaccharides with the substratum.

Therefore, polysaccharides need to be studied and characterized in order to understand and control bacterial adhesion. Different polysaccharides such as cellulose, pullulan, dextran, etc. can form covalent bonds with varying strengths with certain

substrates. Thus identifying these polysaccharides present on the cell surface of a particular bacterial strain can help characterize the adhesive capabilities of the strain.

Atomic force microscopy (AFM) has been extensively applied as a spectroscopy technique for measuring interfacial forces between bacteria and surfaces. In a number of studies, AFM was used to study isolated polysaccharides for their properties. The application of AFM in studying polysaccharides was further extended to study the surface of a live cell for detecting the absence of a particular polysaccharide when the cells are treated with the appropriate enzyme.

The goal of this study was to detect the removal of polysaccharides, present on a cell surface, after treating the cells with appropriate enzyme, using atomic force microscopy. The technique is useful when used with some prior knowledge of possible sugars present on the cell surface.

Prior work done on *Pseudomonas putida* KT2442 using NMR, the EPS present on the cell surface was found to have three possible sugars including cellulose (Camesano and Abu-Lail, 2002). The *Leuconostoc mesenteroides* cells are known to be rich in dextran on their surface (Scott and Gregory, 1998).

The concept used in this study exploits the adhesive nature of bacterial cells which is well known to be due to the polysaccharides present on the cell surface. The difference in the adhesive nature of a cell before and after the enzyme treatment, as observed using AFM spectroscopy, provides information about the changes that the polysaccharides on the cell surface undergo.

2.0 Literature Review

2.1 *Polysaccharides*

Polysaccharides and glycol-substances have emerged rapidly as a subject of interest in the last few years for researchers, mainly because of their application in the field of biotechnology. Despite being built up from very similar building blocks: the pyranose or furanose carbohydrate ring structure, they bear a vast diversity in structural and functional properties. Polysaccharides can be rod-shape molecules such as xanthans, chitosans and alginates, linear random coil-shaped structures such as dextrans and pullulans, or branched structures such as glycogens and amylopectin. Polysaccharides can also be categorized on the basis of charge such as polyanions like alginates, pectins, carrageenans, xanthans and hyaluronic acid; neutral structures like guar, pullulan and dextran, and polycations like dextran derivatives and chitosans (Tombs and Harding, 1997).

Polysaccharides play an important role as structural components of living systems (Dumitriu, 1998) such as in plant cell walls and as storage (store carbohydrates) components such as in seeds (Tombs and Harding, 1997). Other important roles that they are believed to play are that of wound healing agents, anti-microbial agents and in some situations as anchors which fix algae to rocks and thus adhesives. Bacterial polysaccharides are also known to be involved in lectin interactions.

Conformations of common polysaccharides (Tombs and Harding, 1997)

Table # 1

Conformation	**Examples**
Extra-rigid Rod	Schizophyllans, xanthans
Rigid Rod	Alginates, pectins, chitosans
Semi-flexible coil or Asymmetric Rod	Xylans, chitosans, pectins, cellulose nitrate, methyl cellulose, mucin glycoproteins
Random coil	Pullulan, dextran, guar, locust-bean gum, konjac mannan
Globular or highly branched	Amylopectin

The wide application of polysaccharides in the field of biotechnology has triggered a lot of research in understanding the structure and function of various polysaccharides. Polysaccharides are used as a source of oligosaccharides and as enzyme substrates in the determination of enzyme specificity (Sutherland, 1998).

In order to understand the structure various techniques have been employed such as X-ray fiber diffraction (Clark, 1994), small-angle X-ray spectroscopy (Villetti et al., 2000), X-ray photoelectron spectroscopy (Rouxhet et al., 1991), Infrared spectroscopy (Van der Mei et al., 1989), electron microscopy (Hermansson and Langton, 1994), mass spectrometry (Sturgeon et al., 1983), nuclear magnetic resonance (NMR) (Vignon et al.,

1996) and molecular modeling. Due to properties like polydispersity, flexibility and crystallizability X-ray diffraction has not been able to provide enough information about the polysaccharides. Scanning electron microscopy (SEM) has provided with a direct visualization of polysaccharide structure but at the cost of harsh treatment upon the chains. High shearing and surface tension forces on air-drying prior to exposure to high vacuums can affect molecular integrity. The same is true for techniques like TEM (Ransom et al., 1997) and XPS where the sample needs to be in high vacuum environment. TEM can be used to determine mass per unit length of a polysaccharide (Tombs and Harding, 1997). Scanning electron microscopy can be used for studying particulate and composite gels such as starch (Hermannson and Langton, 1994). None of these techniques can provide information on the behavior of the polysaccharides as they exist in nature (Boonaert et al., 2000). Atomic Force Microscopy (AFM) can provide information about polysaccharides under more natural conditions.

With the ability to image objects at the angstrom scale and record force interactions on the order of pico-Newtons (Fisher et al., 1999), AFM has proved to be the best instrument for studying polysaccharides. Not only have the polysaccharides needed not to be in an alien environment but also they can be imaged while attached to their parent cell. The first biopolymer studied through stretching experiments with the AFM was DNA (Smith1992, Lee 1994a, Marko 1994, Smith 1996, Strick 1996). The application was further extended to studying proteins and then to polysaccharides for determining elasticity and length of chains. Since then, AFM has been used extensively in the field of characterizing polysaccharides in a number of ways. Tips modified by

attaching different probes such as specific polysaccharides, proteins and even whole cells are being used to determine their interaction with similar or different entities. In a number of instances stretching experiments have been performed on independent polysaccharide molecules attached to surfaces such as gold and elasticity measurements for the respective polysaccharides (Rief and Gaub, 1997). The same concept has been used for determining the lateral distribution of receptor on a sample surface by mapping adhesion force with a corresponding immobilized at the tip (Rief and Gaub, 1999). AFM has also been used for polysaccharide fingerprinting where the extension-time graphs have been used by increasing the pulling force on the polysaccharide strand with time to see any characteristic behavior for that particular polysaccharide (Marszalek et al., 1998, 1999, 2001; Brant, 1999).

Properties of polysaccharide chains can be determined by measuring parameters like contour lengths, persistence lengths and end-to-end distances of the chain using AFM. For a linear polysaccharide which is not rigid, the most useful representation can be in terms of a worm-like-chain model, which covers the range of flexibilities from stiff rod to a completely random coil. The extent of flexibility can be determined by the ratio of the contour length to the persistence length or simply in terms of persistence length. A persistence length approaching zero (~ 10 Å) indicates the polysaccharide chain is very flexible and exists as a random coil. A persistence length approaching infinity (~ 2000 Å) indicates the chain is a rigid rod.

Bacterial polysaccharides are quite different in function from those of higher plants. They are secreted from the cell to form a layer over the surface of the body and

extend to large distances as compared to the size of the actual body. The growth of these polysaccharides on the surface of a cell is believed to be for protection. The polysaccharides protect the cell body by offering steric repulsion to foreign harmful bodies such as bacteriophage. Polysaccharides also help in preventing dehydration. They also help in protecting cells from the cells of the immune system or phagocytosis by microorganisms. Polysaccharides can also be involved in pathogenicity such as in *Pseudomonas aeruginosa*. Other than these functions these polysaccharides also help in attaching to different surfaces (Frank and Belfort, 1997) and some of the polysaccharides present on a cell surface might be responsible for penetrating into other living bodies.

Besides these characteristics there are other important factors that can influence their structure and thus behavior in a medium. Ionic strength is one of the factors that have been very much investigated for its influence on the conformation of the polysaccharide chains. Hydrodynamic radius of anionic exo-polysaccharides decreases with increasing ionic strength of the surrounding media where the radius remains unaffected for the neutral exo-polysaccharides in similar conditions implying a change in the polymer conformation due to charge screening (Frank and Belfort, 1997).

2.2 Bacterial Adhesion

The importance of bacterial adhesion was first introduced by Claude ZoBell and coworkers in the 1930s. After a silent period of 30 years the subject of bacterial adhesion again became of interest in the early 1970s. And for the last 3 decades many researchers have shown great interest in elucidating the mechanisms of attachment to surfaces and in understanding the influence of attachment on the bacterial cell and on the surface it attaches to.

Bacterial adhesion constitutes the first step toward the formation of biofilms on any surface (Razatos et al., 1998). Some of the driving forces for bacteria to adhere to a certain surface are the presence of nutrients at the interface and protection against toxic conditions. In many cases, however, surfaces of plants and animals remain free of bacteria because their chemistries are unsuitable for adhesive interactions (Rosowki et al., 1992), since they produce toxins or repellants (Keifer and Rinehart, 1986; Todd, 1993) or they continually slough surface layers (Johnson and Mann, 1986). The ability of bacteria to adhere may vary due to the diversity in available substrata for attachment and associated environmental conditions.

2.2.1 Factors affecting bacterial adhesion

The surfaces of substrata and bacteria as well as the medium affect the attachment process. Some surfaces act as better attractants for the attachment where as others are repellant surfaces. Mostly the effort is to identify the nonsticky ones or make a surface resist adhesion. Some of the examples of surfaces where microbial fouling is a

serious problem are ship hulls, water pipelines, heat exchangers and bioreactors. And because of the formation of such microbial mats, gradients in environmental nutrients and low molecular weight substances are often established (Cohen and Rosenberg, 1989). Bacterial colonization may involve changes in cell surface properties that regulate the adhesiveness, such as changes in hydrophobicity that alter the adhesion of benthic cyanobacteria (Shilo, 1989). Also bacterial adhesion can get affected by any changes with the properties of surface with time such as in the case of increased adhesion of *Pseudomonas aeruginosa* on worn rigid gas permeable lenses (Bruinsma and van der Mei, 2003). In another case roughness and topography of the surface affected the bacterial attachment (Boyd and Bhakoo, 2002; Shellenberger and Logan, 2002). In a number of studies researchers have attempted to relate attachment to physicochemical properties of substrata such as net surface charge (Feldner, 1983; MacRae and Evans, 1983), surface free energy (Van Pelt and Arends, 1985), critical surface tension (Dexter, 1979; Becker and Wahl, 1991), surface hydrophobicity (Fletcher and Loeb, 1979; Fletcher and Marshall, 1982; Paul and Loeb, 1983; Vadillo-Rodriguez and van der Mei, 2003) or work of adhesion for water (Pringle and Fletcher, 1983). Most of these parameters can be determined using contact angle information about the surface. Medium in which the bacteria are suspended may play an important role in deciding the success of bacterial attachment.

The bacterial surface also plays an important role in deciding the fate of bacterial attachment. Properties like motility (Camper, 1993), growth rate (Mercer, 1993), cell shape and size (Weiss, 1995), growth phase (Fletcher, 1977), cell elasticity,

electrostatics (Velegol and Logan, 2002) and length of lipo-polysaccharides present on the cell surface (Burks et al., 2003) affect the attachment. The properties of a cell such as shape, size and motility depend on the growth phase of the cell. *Pseudomonas putida* KT2442 changed from cylindrical to spherical as the cells reach stationary phase of their growth (Eberl et al., 1997). Size and shape of a bacterial cell affect its attachment to a certain surface (Weiss et al., 1995). Cell surface hydrophobicity may facilitate attachment to soil or sediment particles (Stenstrom, 1989; Vadillo-Rodriguez and van der Mei, 2003).

Other than these factors the heterogeneity associated with the bacterial surface, even on a single cell is tremendous (Abu-Lail and Camesano, 2002). Numerous macromolecules interface with the surrounding medium, and these vary in composition and quantity from species to species and from strain to strain and with environmental conditions and physiological processes. Certain groups on the surface macromolecules of a bacterium may help in attaching to a particular surface and for the same bacterium some other groups present on the macromolecules would help in the attachment with a different surface with a different degree of adhesion (Doyle, 1982). These surface polymers may prevent adhesion by binding water or through steric repulsions. Among the surface polymers extracellular polysaccharides, proteins and lipo-polysaccharides are known to play important part in attachment process at different stages (Allison and Sutherland, 1987). EPS exist in the form of loosely bound capsule on the top of the LPS layer which in turn is an extension from the surface of a bacterial cell with O-antigens on top of the LPS layer (Kastowsky, 1992). O-antigens constitute an important part of

the LPS layer and decide the hydrophilicity of the cell surface (de Maagd, 1989). Absence of O-antigens, which may sometimes be the case, ensures cell surface hydrophobicity. Extracellular polysaccharides assist in forming biofilms by binding with EPS on other cells and also help in bacterial adhesion. EPS can be a response to the process of attachment (Allison and Sutherland, 1987) or can be present before adhesion and actually be helping in the attachment as in the case of marine *Hyphomonas* sp. (Quintero and Weiner, 1995). Alginate (EPS) from *Pseudomonas aeruginosa* helps in binding cells together and to the epithelial cells of the respiratory tract (Ramphal, 1987; Pederson, 1992). In another case alginate produced by *Pseudomonas fluoroscens* strongly inhibited adhesion (Pringle, 1983). The variation in behavior of the same polysaccharide was due to the chemical structure in which it existed on two different types of cells i.e. because of different degree of acetylation and different ratio of mannuronic acid to guluronic acid in its structure in two different conditions (Fett, 1989; Conti, 1994).

In a flow system, velocity of the flow, cell concentration and solution ionic strength affect bacterial transport to the site of attachment on a substratum (Gannon and Alexander, 1991; Li, 1996; Camesano and Logan, 1998). Bacterial transport is also affected by the relative amounts of monovalent and divalent cations present in the solution (Seaman, 1995). Presence of surfactants or surface charge modifying chemicals can also affect bacterial transport in porous media (Li, 1996; Sharma, 1985). Another physical parameter that can affect the transport of motile bacteria is temperature such that motile bacteria are rendered immobile at low temperatures (McCaulou, 1995).

2.2.2 Interaction forces during bacterial adhesion

Two theoretical approaches derived from colloid and surface chemistry have been applied to studies of bacterial attachment in order to evaluate and understand the interactions that control adhesion. These theoretical approaches are The DLVO theory, which takes into account the attractive van der Waals interactions and repulsive electrostatic interactions; and thermodynamic models, in which the adhesive interaction is treated as an equilibrium process and is described in terms of the surface free energies of the bacterium, substratum and separating liquid.

The DLVO theory accounts for the net surface charges on the surface bacteria and substrata. This electrostatic force usually exists as repulsion between the two bodies because of negative charge present on the surfaces in natural systems. The other force that acts against this repulsive force is van der Waals attraction. Under certain circumstances this type of force can be repulsive depending on relative magnitudes of an important parameter, the Hamaker constant, of the two surfaces interacting and of the separating liquid. van der Waals forces do not depend on the ionic strength and pH of the medium (Israelachvili, 1992). The balance of these two long range forces predicts two separation distances from the stationary surface at which the approaching colloidal particle (or bacterium) can attach to the surface called primary minima and secondary minima.

The primary minimum offers maximum attraction to the approaching colloid and results in irreversible attachment if once accomplished. Secondary minimum deposition results in reversible attachment such that the pull between the two bodies can

be overcome at the expense of some extra energy by the colloidal body which in the case of a bacterium can come from its motility.

Otherwise motility has been found to assist in bacterial adhesion by facilitating the transport of bacteria to the site of adhesion (Wenyuan and Hong, 2002; Vigeant and Ford, 2001). Apart from the classical DLVO theory extended DLVO theory was introduced which incorporated two extra features of bacterial cells i.e. the steric interactions due to surface polysaccharides and acid base interactions. In a study *E. coli* cells were attached to the AFM tip to probe surfaces with different degree of hydrophilicities and the forces of interaction have been compared with the extended DLVO model (Ong et al., 1999).

$$F_{DLVO} = F_v + F_e \ldots (1)$$

$$F_{DLVO} = -\frac{Aa}{6h^2} + \pi\varepsilon\varepsilon_o a(\varphi_1 + \varphi_2)^2 \frac{2k}{1 - e^{-2kh}} \ldots (2)$$

ε = Relative dielectric permittivity of water

A = Hamaker constant

ε_o = Permittivity of vacuum

a = Radius of tip

φ_1 = Surface potential of tip

φ_2 = Surface potential of bacterium

k = Inverse Debye screening length

h = Separation distance between tip and bacterium

The above model of DLVO assumes plate and sphere system with tip (as shown in **Figure 3**) as a sphere and bacterium as a flat plate. The spheres in following figure represent imaginary spheres with the same radius as that of the tip.

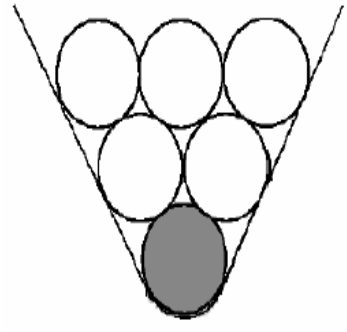

Figure 1: Representation of a tip in the form of number of imaginary spheres with the same radii as that of the tip

Some of the studies done to characterize AFM cantilever contend that a tip should be considered to have two spheres of different radii interacting with the sample (Bykov, V. A. et al., 2003).

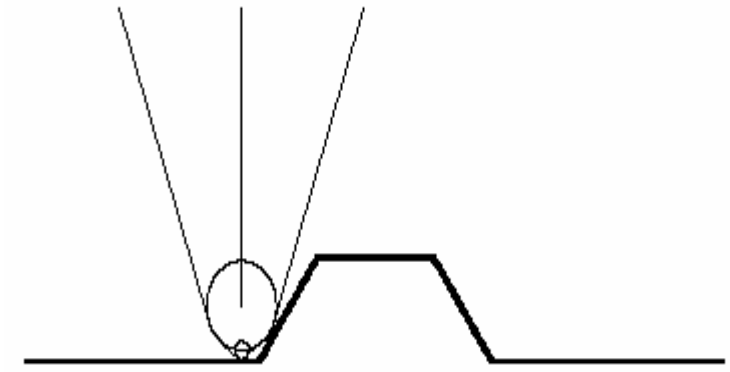

Figure 2: AFM tip with its point acting as a sphere on a flat surface

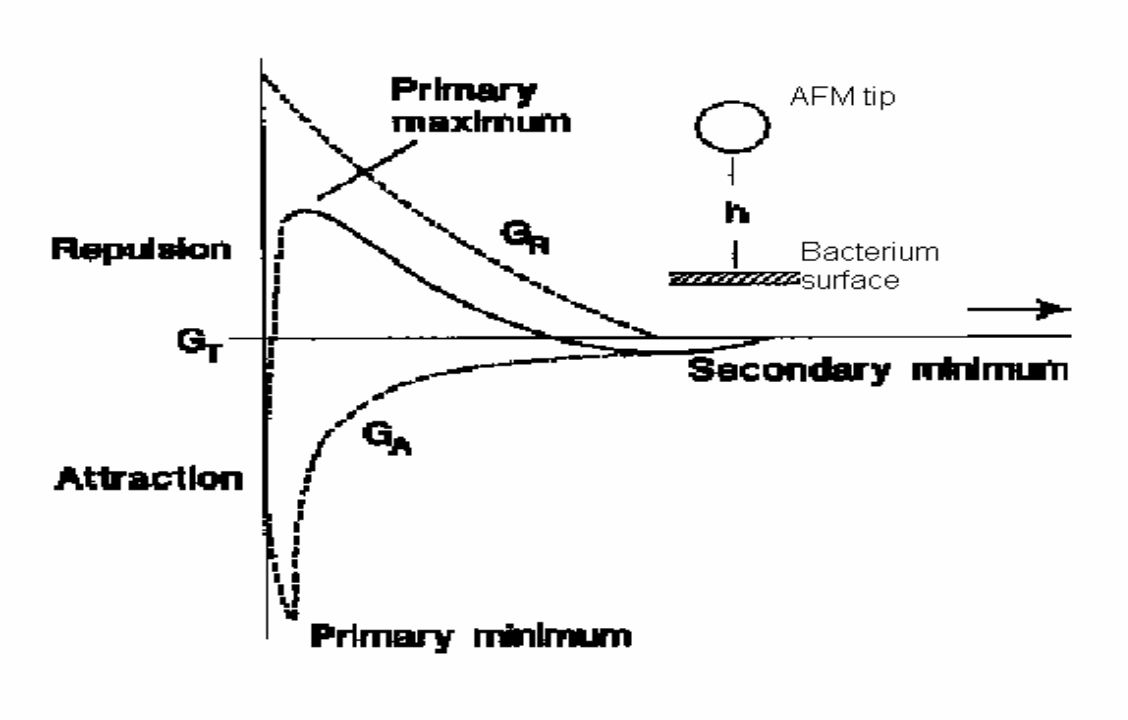

Figure 3: Forces of interaction between an AFM tip and a bacterial cell surface as the distance between the two decreases.

Another model is a sphere-sphere model. This model describes tip-bacterium system more closely since the tip radius is approximately same as that of the bacterium (Eq 3) (Abu-Lail and Camesano, 2003).

$$F_{DLVO} = \frac{2\pi a_1 a_2 n k_B T}{(a_1 + a_2)\kappa^2}(\Phi_1^2 + \Phi_2^2)\left(\frac{2\Phi_1\Phi_2}{\Phi_1^2 + \Phi_2^2}\ln\left(\frac{1 + \exp(-\kappa h)}{1 - \exp(-\kappa h)}\right) + \ln\left[1 - \exp(-2\kappa h)\right]\right) + \frac{Aa_1 a_2}{6h(a_1 + a_2)(1 + 11.12\, h/\lambda c)} \quad ...(3)$$

a_1 - Radius of tip

a_2 - Radius of bacterium

Φ_1 - Reduced potential of tip

Φ_2 - Reduced potential of bacterium

DLVO theory does not work for most of the systems especially for bacterial cells where biopolymers present on the cell surface play an important role in the bacterial adhesion. These steric repulsions due to extended biopolymers on bacterial surface are mostly very long range forces which hide all the other forces and factors included in the DLVO model. In the case of steric repulsions the bacteria adhere with the help of extending polysaccharides instead of the van der Waals attraction. Electrostatic forces may come into play if the polymers are charged. All other factors such as surface heterogeneity, acid-base interactions and dynamic interactions between double layers do not come into picture since these are only applicable in shorter ranges of interaction. Thus another model was developed which depends on two adjustable parameters that are length of the polymer brush (L_o) and grafting density of the polymer brush (Γ).

$$F_{steric} = 50\,KTaL_o\Gamma^{3/2}e^{-2\pi h/L_o} \quad ...(3)$$

K = Boltzmann constant

T = Temperature (298^{o} K)

a = Tip radius (250 nm)

L_o = Polymer brush length (nm)

Γ = Grafting polymer density (m^{-2})

h = Separation distance (nm)

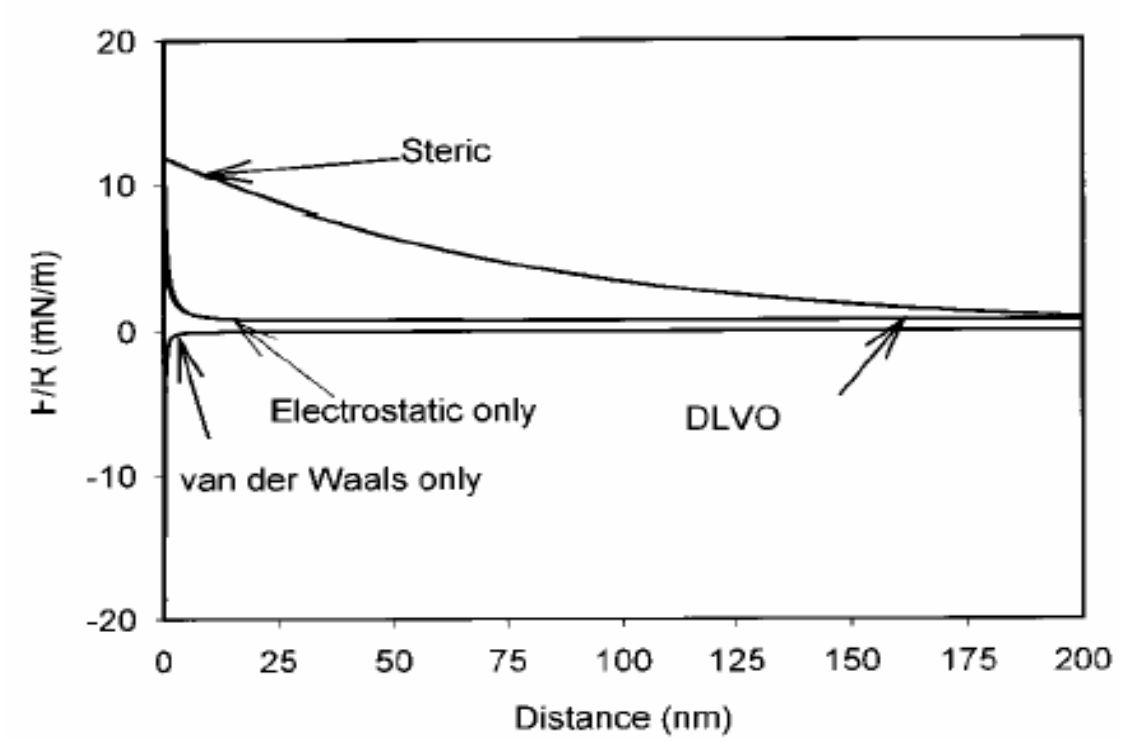

Figure 4: Normalized force comparison between the three main possible forces of interaction. Steric repulsion being higher than van der Waals and Electrostatic forces and also extends to longer range comparatively. Adapted from (Camesano, T. A. and Logan, B. E., 2000)

In the thermodynamic theory attachment is viewed as a spontaneous change, which is accompanied by a decrease in free energy of the system. To test this theory experimentally, it is necessary to determine values for interfacial free energies at the bacterium and substratum surfaces, and these are generally estimated indirectly by measuring the contact angles of liquids on the test substrata and on lawn of bacterial cells (Fletcher and Marshall, 1982; van der Mei et al., 1991).

Some of the studies have found that bacterial attachment data are inconsistent with thermodynamic predictions, but in other cases results cannot be explained by this model (Bellon-Fontaine et al., 1990). The theory fails to describe the bacterial adhesion process firstly because of the assumption of an equilibrium situation and secondly because of difficulty in identifying all components of the process due to chemical complexity of bacterial attachment surfaces. Also determining exact values for the required parameters such as bacterium surface free energy is extremely difficult (van der Mei, 1991).

2.3 Atomic Force Microscopy (AFM)

Atomic Force Microscope (AFM) has made possible a number of imaging and spectroscopy tasks since its invention which happened only about 20 years ago. As discussed earlier all other imaging and spectroscopy techniques relied upon certain conditions to work in such as high vacuum or the sample to be conducting, whereas AFM can work without any such conditions. AFM can work in a number of different modes (Tapping mode, contact mode and non contact mode) making possible to image a variety of samples with different degree of softness such as soft biological cells in their living state (Yao, X. et al.,2002).

2.3.1 Principles of AFM

An AFM consists of a sharp tip, attached to a cantilever, which rasters over the surface of the sample in a bound scan area and the movement of the cantilever, as the tip moves across the surface, is recorded to produce the image of the sample. The movement of the cantilever is recorded with the help of a laser beam which is shot from the top of the microscope head and shined on the back of the cantilever and as it reflects from the cantilever the beam hits the adjustable mirror and then the fixed mirror and finally enters the position sensitive detector (**Figure 5**). This special photodiode gives the information about cantilevers position to compiler to generate the image of the surface of the sample. The position sensitive detector consists of a scanner piezo tube which is very sensitive to changes in applied voltage and it responds by contracting and expanding to minute changes in voltage. This sensitivity is used to record x, y and z

position of the cantilever end. The four elements of the quad photodiode combine to provide different information depending on the operating mode. In all modes the four elements combine to form the SUM signal. The amplified differential signal between the top two elements and the two bottom elements provides a measure of the deflection of the cantilever. This differential signal is used directly in contact mode AFM. For tapping mode the signal is fed into an RMS converter or phase module if attached. For Lateral Force Microscopy the amplified differential signal between the sum of the two left photodiodes and of the two right photodiodes provides a measure of the torsion in the cantilever.

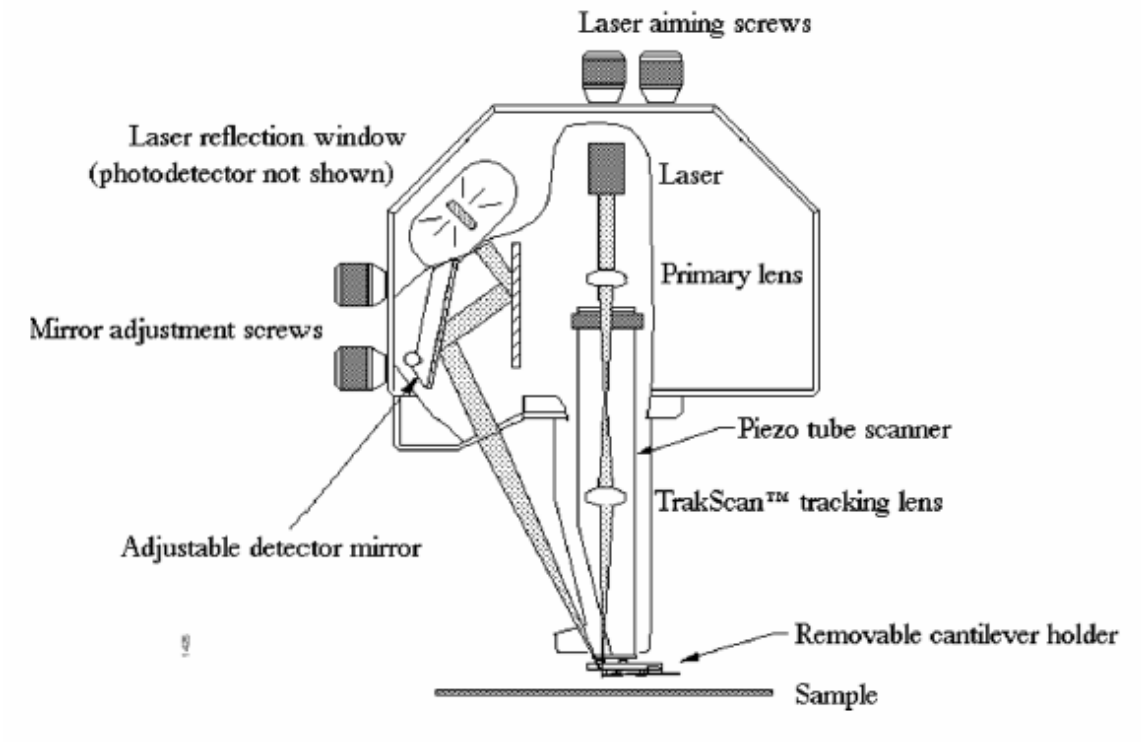

Figure 5: Microscope head and its parts

Digital Instruments (Training Notebook)

As pointed out earlier one of the main advantages of AFM over other electron microscopic techniques are its ability to look at softer bodies such as cells, tissues and biomolecules such as proteins, nucleic acids etc. and also that AFM can image these entities in air as well as liquid. The tip that moves across the sample plays an important role in depicting the right picture. The AFM works with two different types of holders for carrying the tips for air and liquid. The type of tip that works well in air may not work that well in liquid. Following is a chart showing the type of tips suitable for different purposes. The resolution of an image captured by AFM depends on the radius of the tip. The radius of the tip should be smaller than the features on the sample to get a well resolved image. Depending on the kind of surface under observation the tips with different spring constant are chosen. Use of AFM in contact mode is generally avoided on biological samples due to their softer surface which can be damaged by friction between tip and surface while imaging. Thus AFM is used in tapping mode on biological samples and this allows the samples to be imaged unharmed and in their living state. Samples can be imaged very well in air using AFM but it is not possible to get good force curves on those samples in air due to high capillary forces that come into play because of thin water films present on the tip and on the sample surface. These capillary forces being so large hide the actual force of interaction between the tip and the sample and thus make capturing force curves in air useless. AFM's ability to look at samples under liquid makes it possible to capture actual force curves. Capturing force curves for bacterial cells in water using AFM makes it more realistic since bacterial

adhesion takes place essentially in liquid systems in nature. Thus AFM gives a closer picture of the actual interaction forces that a bacterium experiences during the attachment process. The tips used are mostly silicon nitride tips, in case of bacterial cells, which imitate sand particles very well. Carbon nanotubes have been used as probes and have resulted in improved lateral resolution of the smaller features on a sample (Rozhok et al., 2003). The carbon nanotubes tips are widely accepted for their small diameter, high aspect ratio, large Young's modulus, mechanical robustness, well defined structure and unique chemical properties (Hafner et al., 2001). Other silicon nitride cantilevers with oxidation-sharpened silicon tips have been made and used to get better resolution of softer samples such as cells. These tips are sharp and have a low spring constant (Grow, Randal et al., 2002).

Table # 2

Samples	AFM type		AFM Mode		Experiment		First Choice Probe (Model)
	MultiMode	Bioscope/ Dimension	TappingMode	Contact Mode	Air	Liquid	
Biomolecules (Nucleic Acids, Proteins, Lipids, Carbohydrates,...)	x		x		x		OTESP or TESP
	x		x			x	NP-S or NP-STT or OTR4
Cells		x	x	x		x	(D)NP or tipless probe with attached sphere
Tissues	x	x	x	x		x	(D)NP or (D)NP-S
	x	x	x		x		TESP
Biomaterials	x	x	x		x		OTESP or TESP or FESP
	x	x	x			x	(D)NP-S
Force Measurements	x	x				x	(D)NP or OTR4

Digital Instruments (Choosing AFM probes for biological applications)

www.veeco.com

2.3.2 Applications of AFM

The introduction of the atomic force microscope (AFM) and its application to biol. surfaces has offered new possibilities to obtain microscopic, physicochemical properties of bacterial cell surfaces (Vadillo-Rodriguez et al., 2003). AFM has been used to find relation ship between microscopic and macroscopic cell surface properties (Vadillo-Rodriguez et al., 2003). Besides imaging AFM provides quantitative information about the captured images as well which can be very useful in some instances. By applying varying shear/lateral force to detach individual bacterial cells from various substrata of different surface topographies, relation between changes in surface roughness and bacterial attachment was found on quantitative basis (Boyd et al., 2002). A similar study has been done using AFM to find relation between surface charge heterogeneity and the deposition rates of colloids during their transport in porous media (Shellenberger and Logan, 2002). AFM has been used to understand the role polysaccharides present on bacterial cells play by offering steric hindrance and blocking the long range attractive forces between bacteria and substrata (Razatos et al., 2000). Understanding bacterial adhesions on biomaterials has been another important step made possible with the help of AFM. Modified AFM tip with *E.coli* cell has been used to get force interaction patterns with different kind of substrata such as mica, hydrophilic glass, hydrophobic glass, polystyrene and Teflon which has helped in

understanding the kind of interactions between *E.coli* strains with different could-be biomaterial surfaces (Ong Yea-Ling, et al., 1999). AFM has been used successfully in determining factors responsible for bacterial adhesion in certain cases. Razatos A. et al., in 1998 found that adhesion force is affected by the length of core lipopolysaccharide molecules present on the E. coli cell surface and by the production of the capsular polysaccharide, colanic acid. Similarly in a number of other instances AFM has helped in understanding factors affecting attachment process such as in *Bacillus mycoides* spore adhesion (Bowen et al., 2002). Other than recording topography of the sample AFM can also help in detecting the contamination on the sample by phase imaging technique (Pauli et al., 2003; Fasolka et al., 2001; Behrend et al., 1999).

With its ability to scan small areas, of the range of few nanometers, of the sample AFM has found its application in the field of carbon nanotubes and in other non biological fields as well. AFM has been used in contact force mode to study the structures of carbon nanotubes and to cut carbon nanotubes adsorbed on a glass slide (Singjai et al., 2002). AFM in combination with scanning capacitance microscopy was applied to study the two-dimensional carrier profile of semiconductor devices (Chao, Kuo-Jen et al., 2001). AFM has been used to characterize inorganic particles. In this study of characterization the roughness measurement was not of much help since the surface roughness of particle sample exceeded AFM limit but phase images from AFM helped in differentiating solid from hollow particles. The force spectroscopy from AFM was also able to tell the difference between the solid and hollow particles (Park, 1999). AFM has been used in a variety of studies covering different kind of samples for

ensuring heterogeneity on the surfaces. Phase imaging and nanoindentation techniques of AFM have been used to study the heterogeneity in polymeric materials (Gu, Xiaohong et al., 2000). AFM has been used to investigate the heterogeneity and flexibility of human ocular mucins and their subunits (Round et al., 2002). Heterogeneity in biopolymers on the same bacterium and among several bacteria has been found with the help of AFM (Camesano and Abu-Lail, 2002). AFM has also been used in mapping regions of heterogeneity in PEA/PS film by allowing the film to react in a low pH environment and analyzing by AFM (Raghavan et al., 2001).

Other area where AFM has been successfully is the in-situ studies and it has been more helpful than many other techniques like TEM and SEM in certain cases. AFM coupled with XRD has been used to investigate mineral-surface heterogeneity and heterogeneous systems in situ (Liu, Chen et al., 2003). The kinetics and mechanism controlling dissolution from the (100) cleavage face of KBr single crystals in Methyl-CN solutions have been identified by using a novel integrated electrochemical/AFM probe and a scanning electrochemical microscope (SECM) (Macpherson, Julie et al., 1996). AFM has also been more helpful in studying non crystalline material than any other available techniques (Liu, Chen et al., 2003; Kowalewski, Tomasz, 1996).

3.0 Materials and Methods

3.1 Culture

The experiments were performed on two bacterial strains *Pseudomonas putida* (KT2442) and *Leuconostoc mesenteroid* (NIRC1542). KT2442 was provided by M. Röthlisberger (Swiss Federal Institute of Technology, Zürich). KT2442 is a rifampicin-resistant, plasmid-cured derivative of *P. putida* mt-2 (Eberl, Molin et al., 1996; Bagdasarian, Timmis et al., 1981). KT2442 is a rod shaped bacterium and changes to spherical geometry as it reaches the stationary phase of its life cycle (Eberl, Molin et al., 1996). KT2442 has been found to be motile in low ionic strength water systems (Samanta and Jain, 2000). KT2442 belongs to the gram-negative category of bacteria and thrives in aerobic environment. Being a gram negative bacterium the cell has a layer of lipopolysaccharide chains and protein on the surface of the cell **(Figure 6)**. These LPS chains may secrete another layer of exopolysaccharide chains on top of them which play an important role in the attachment of bacterium to surfaces. The production of this loose layer of polysaccharides on LPS can also be a result of the bacterial adhesion.

The contact angle of water on a lawn of KT2442 cells is 24.5±3.4^{o} indicating that the cells are hydrophilic in nature (Camesano, Logan et al., 1999). The zeta potential of the cell surface is normally considered as the surface potential. The zeta potential for the cells, when no polysaccharides present on the surface, is about (-16)-(-20) mV in 0.1 mM MES buffer (pH 7) (Camesano and Logan, 2000; Abu-Lail and Camesano, 2002).The zeta potential of the surface polymers for KT2442 was found to

be (-3)-(-4) mV (Abu-Lail and Camesano, 2002), indicating that the polymers present on the surface are not highly charged and they are only slightly negatively charged and this negative charge can be due to phosphate or carboxylic groups present on the polysaccharide chains. Also the iso-electric point for KT2442 cells was found to be at pH 2.3 (Abu-Lail and Camesano, 2002).

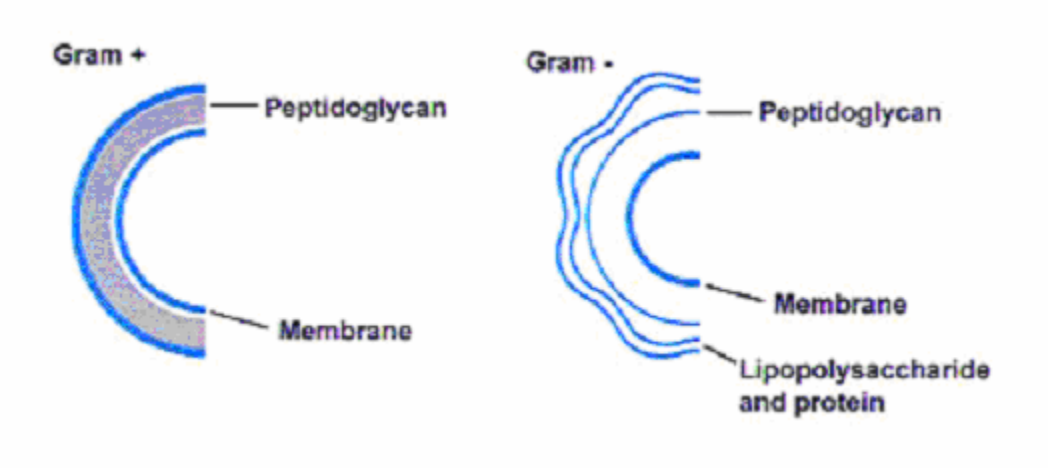

Figure 6: Comparison of gram positive and gram negative bacteria cell surface. Gram positive possess a thicker cell wall consisting of peptidoglycans whereas gram negative have a thin cell wall made up of peptidoglycans and mostly consists of the LPS and protein brush. Adapted from Brock & Madigan "Biology of Microorganisms" 5th Ed., 1988

The other strain used for the experiments was *L. mesenteroides* NIRC1542. The microbe was provided by Dr. Hui Zhang (Research institute of Biological resources, National institute of Advanced Industrial Science and Technology). The strain is one of the dextran producing strains of the *L. mesenteroides* family.

3.2 Media and other solutions

The general medium of growth used for KT2442 was tryptic soy broth (TSB, purchased from Sigma). The medium was made by dissolving 30g of TSB powder in 1 liter of Milli-Q water. The solution was sterilized at 121^{o} C for 15 minutes before it was used. The medium was used for pre-culturing of KT2442 prior to growing the cells in its specific media. TSB provides all the nutrients needed for the growth and serves as a universal media for all bacterial cells.

The specific media used for growing KT2442 was the benzoate solution of M9 buffer. The M9 buffer (Maniatis et al., 1982) was made by dissolving Na_2HPO_4 (7g), KH_2PO_4 (3g), NaCl (0.5g) and NH_4Cl (1.0g) in 1 liter of Milli-Q water. The pH of the solution was adjusted to 7.0-7.2. The solution was then sterilized at 121^{o} C for 55 minutes. 5mM solution of benzoate solution was made in M9 buffer by adding and dissolving 0.55 g of Benzoic acid (purchased from Sigma) in 900 ml of M9 buffer. This solution was then used as the selective media for growing KT2442 cells.

Other ingredients were added to the specific media in order to accelerate the growth of the cells and also to prevent contamination of the cell culture. KT2442 strain being resistant to the antibiotic, rifampicin, gives an advantage of adding rifampicin to prevent the contamination in the media. 1 ml of rifampicin was added to 100 ml of the specific media (Nüβlein et al., 1992). Pseudomonas goodies were added to the media to accelerate the growth of the cells. The goodies consist of 50 ml of salt solution, 25 ml of 1M $MgSO_4$ solution and 25 ml of 36mM $FeSO_4.7H_2O$. The salt solution consisted $CaCO_3$ (2g), MgO (10.75g), $FeSO_4.7H_2O$ (4.5g), $ZnSO_4.7H_2O$ (1.44g), $MnSO_4.4H_2O$

(1.12g), $CoSO_4.7H_2O$ (0.28g), $CuSO_4.5H_2O$ (0.25g), H_3BO_3 (0.02g) and HCl (51.3ml) in 1liter of Milli-Q water (Nüβlein et al., 1992). 250 μg of goodies were added to 100 ml of the specific media. This composition of Benzoate solution, *Pseudomonas* goodies and rifampicin was used as the final media for growing KT2442 cells by inoculating with 1 ml of the pre-cultured cells in TSB. The cells were grown to an absorbance of 0.6 @ a wavelength of 600nm.

For growing *L. mesenteroides* MRS solution was prepared by dissolving 55g of MRS powder in 1 liter of Milli-Q water. The solution was sterilized at 121^oC for 15 minutes in the autoclave. The cells were grown to the final absorbance of 0.9 @ a wavelength of 600nm.

EDC (purchased from Pierce) solution was used for treating bacterial cells in the process of attachment to glass slides. EDC solution was prepared by adding 0.192 g of EDC powder to 10 ml of Milli-Q water. The resulting 100mM solution was then adjusted for a pH of 5.5. The carboxyl groups present on the cell surface reacted with EDC to form an unstable intermediate (O-acylisourea) (Garabarek and Gergely, 1990; Staros, Swingle et al., 1986).

NHS (purchased from Pierce) solution was used for treating bacterial cells and preparing them for attaching to glass slides. NHS solution was prepared by adding 0.0879g of NHS powder to 10 ml of Milli-Q water. The resulting 40mM solution was then adjusted for a pH of 7.5. NHS reacted with the unstable intermediate by undergoing nucleophilic substitution by the amino group of the aminosilane compound (Garabarek and Gergely, 1990; Staros, Swingle et al., 1986).

The viability test on KT2442 cells have been performed, after they are treated with EDC/NHS in another study and they were found to be unaffected (Camesano and Logan, 2000).

MES buffer was needed for the washing steps during the enzyme treatment. MES solution was prepared by adding 4.7 g of MES powder to 1 liter of Milli-Q water. The resulting 20mM solution was adjusted for a pH of 6.44.

Cellulase stock solution was needed for the cellulase treatment. Cellulase solution was prepared by adding 0.1 g of cellulase (purchased from Sigma) powder to 25 ml of Milli-Q water. The solution was stirred overnight and passed through a 0.45 μm syringe filter and stored as a stock solution to be used later.

Dextranase stock solution was prepared for the dextranase treatment of *Leuconostoc* mesenteroides cells. 3 mg of dextranase powder (purchased from Sigma) was added to 10 ml of Milli-Q water. The solution was stirred overnight and passed through a 0.45 μm syringe filter and stored as a stock solution to be used later.

3.3 Sample preparation

After KT2442 cells were grown the required absorbance of 0.6 @ 600, the cells were prepared for attachment on the clean glass slides for AFM experiments.

3.3.1 Cleaning glass slides

The glass slides (micro slides, purchased from VWR) were treated with a mixture of 30 ml of HCl and 10 ml of HNO_3 acids for 25 minutes. The slides were further treated with a mixture of 40 ml of H_2SO_4 and 10 ml of H_2O_2 for 25 minutes after

rinsing the slides with lots of Milli-Q water (Graber, Natan et al., 1995). The slides were rinsed with water and finally the clean glass slides were stored under Milli-Q water in a beaker for later use.

3.3.2 Cell Attachment

The clean glass slides were treated with methanol for 10 minutes. Methanol was replaced with 10 ml of Aminosilane solution. The Aminosilane solution was prepared by adding 1 ml of 3-aminopropyl dimethoxysilane (purchased from Aldrich) and 9 ml of methanol (purchased from Fisher Scientific). The slides were allowed to be in this Aminosilane solution for 15 minutes. The Aminosilane solution was replaced with methanol and the slides were kept in methanol until the bacterial solution was ready to be poured on the slides (Graber, Natan et al., 1995).

The bacteria on the other hand were centrifuged at 6000rpm (1000g) for 15 minutes. After the cells were spun down, the supernatant was replaced with equivalent amount of Milli-Q water. The cells were resuspended in 9 ml of water and treated with 300 µl of EDC (1-Ethyl-3-(3-dimethylaminopropyl)-carbodimide) for 15 minutes. The cells were further treated with 300 µl of NHS (N-Hydroxysulfosuccinimide) for 15 minutes. The cells were now ready to be poured on the Aminosilane treated slides. 18 ml of the cells treated with EDC and NHS were added to the petri dish containing treated glass slides. The attachment process between the cells and glass slides was

allowed to take place for 9 hrs on a shaker table at 70 rpm (Garabarek and Gergely, 1990; Staros, Swingle et al., 1986).

The following reactions take place upon the addition of EDC and NHS to the cells:

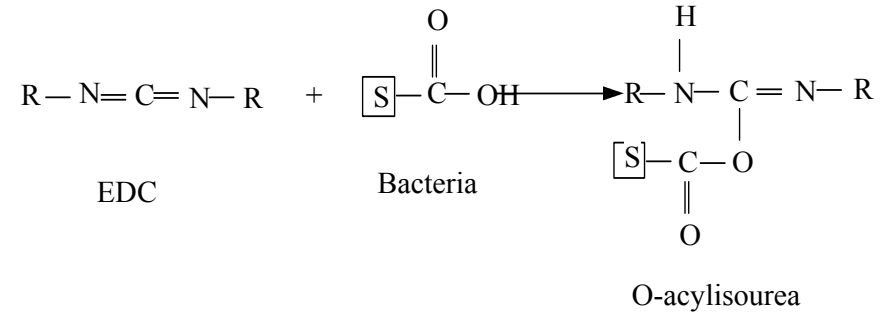

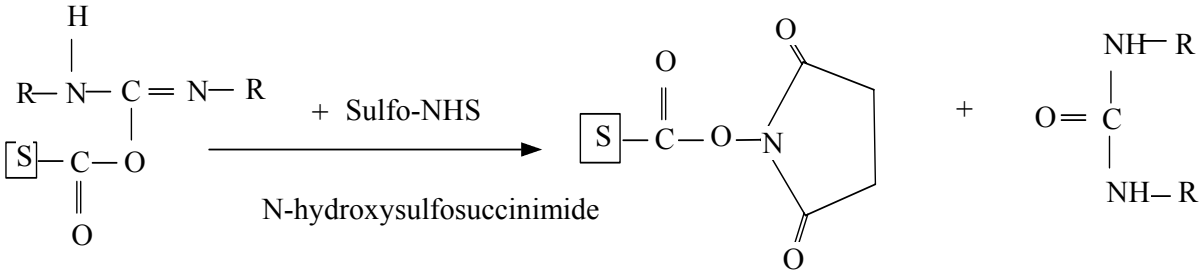

Figure 7: EDC reacts with surface carboxylic groups of bacterial cells to form an intermediate which further reacts with Sulfo-NHS to form a complex that can readily bind to silanized glass slide

The stable intermediate formed further reacts with the silanized glass slides to form the covalent bond and thus the cells become chemically attached to the slide. The reaction that takes place between the intermediate compound and the glass slide is as follows:

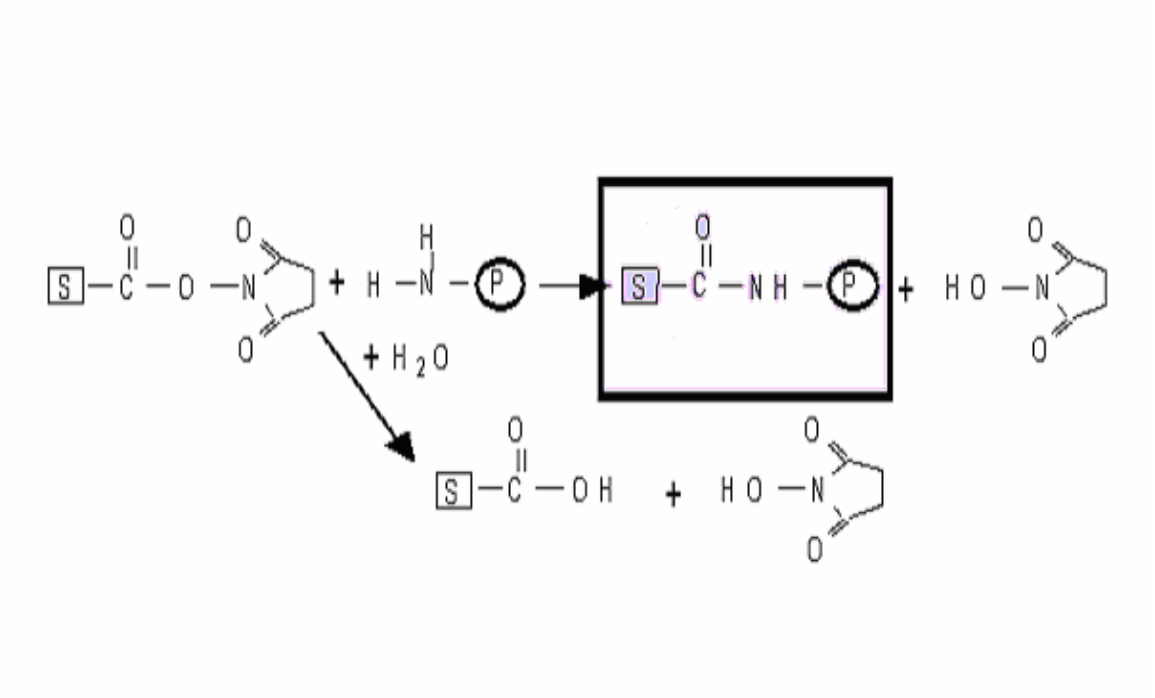

Figure 8: The bacterium forms a peptide bond with the glass slide (P) as shown in the reaction.

3.3.3 Enzyme Treatment

20 ml of the KT2442 cells grown to the absorbance of 0.6 were centrifuged at 6000rpm (1000g) for 15 minutes and the supernatant was replaced with an equivalent amount of the MES buffer. The cells were resuspended and again centrifuged. This step was for washing the cells with the MES buffer. The cells were resuspended in 18.75 ml of MES buffer. 1.25 ml of cellulase solution from the cellulase stock solution was added

to this cell-buffer solution. The final concentration of cellulase in the solution was 250 μg /ml. The solution was set for shaking at 50 rpm on the shaker table for 60 minutes. After the cells were treated with enzyme, the cells were again washed with the MES buffer. The cells were centrifuged at 6000rpm for 15 minutes and the supernatant was replaced with 20 ml of the MES buffer. The cells were resuspended and again centrifuged in the same fashion. The cells were now ready for the attachment procedure. This procedure was modified, for the present system, from the one developed in another study (Frank, 1999)

3.3.4 AFM Experiments

The glass slides with attached bacterial cells were analyzed using Atomic force microscopy (Dimension 3100). The slides were placed on the stage right under the microscope head. The tip used was silicon nitride tips for working in liquid. The tip was mounted on the microscope head and laser was aligned at the back of the cantilever. These tips had a radius of 250 nm and had a typical resonant frequency of about 8 KHz. The sample was scanned in both directions a number of times to find and locate an attached cell on the slide. Several trial force curves were captured before bringing the cell to the center of the scan area. The force curves captured on the clean area of the slide were used to check for artifacts, if any, due to optical interference or distorted tip. Finally the imaged were captured by bringing the located cells to the center of the scan area. The scan area was magnified in order to ensure that the force curves were being captured on the center of the cell. For each cell captured 10-15 force curves were

captured by dropping the drive amplitude to zero while capturing the force curve. 4-6 cells were captured for the cells treated with cellulase and for the untreated cells.

3.3.4.1 Analyzing Force Curves

The files captured on AFM were exported as ASCII data files and the force curves were constructed. The deflection-distance curves obtained from the AFM were converted into force curves by multiplying the displacement by the spring constant of the cantilever **(Figure 9(a))**.

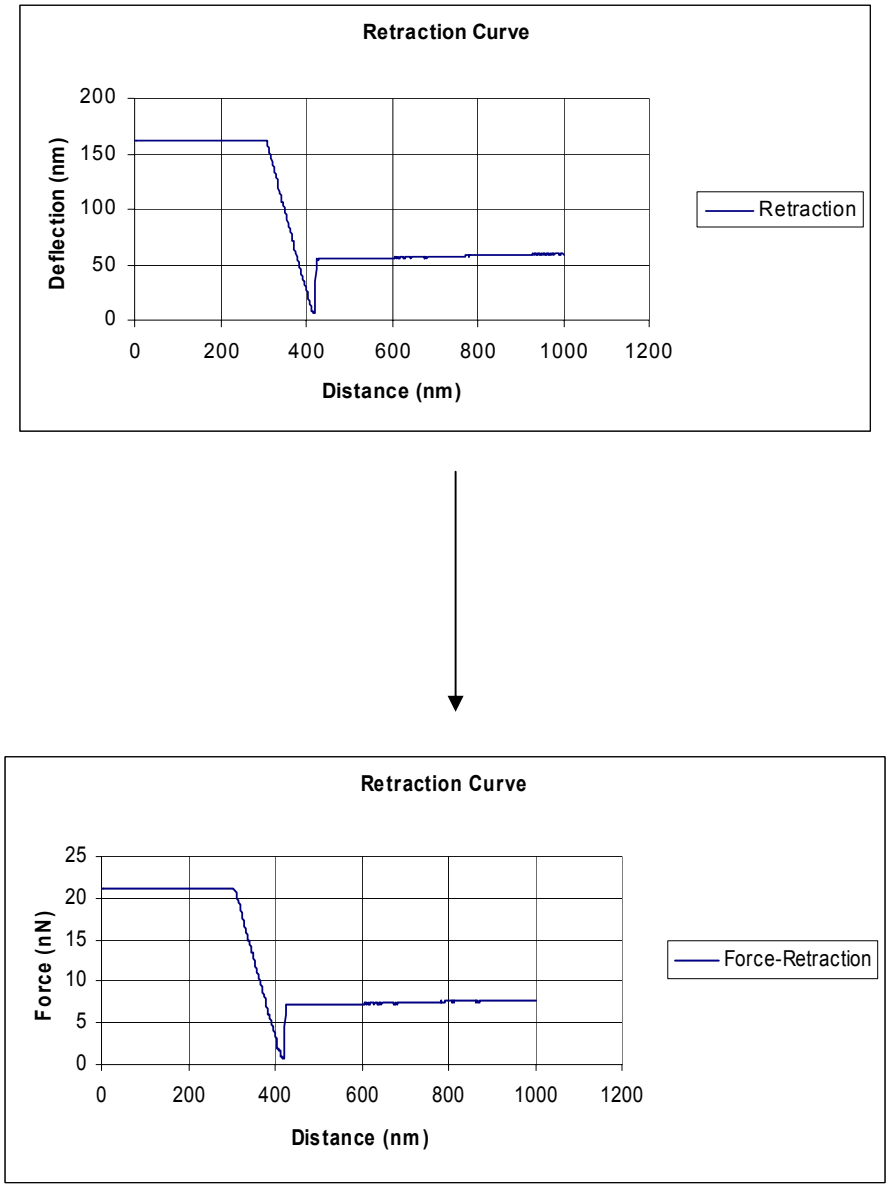
Retraction Curve
Deflection (nm)
200
150
100
50
0
0
200
400
600
800
1000
1200
Distance (nm)
Retraction
Retraction Curve
Force (nN)
25
20
15
10
5
0
0
200
400
600
800
1000
1200
Distance (nm)
Force-Retraction

Figure 9(a)

These force curves were then zeroed to exclude the force measurements made by the tip after it stopped indenting into the sample surface. This was done by adjusting the slope to pass though the origin as well as the curve was adjusted vertically so that the constant-deflection region of the curve rests at zero vertical height.

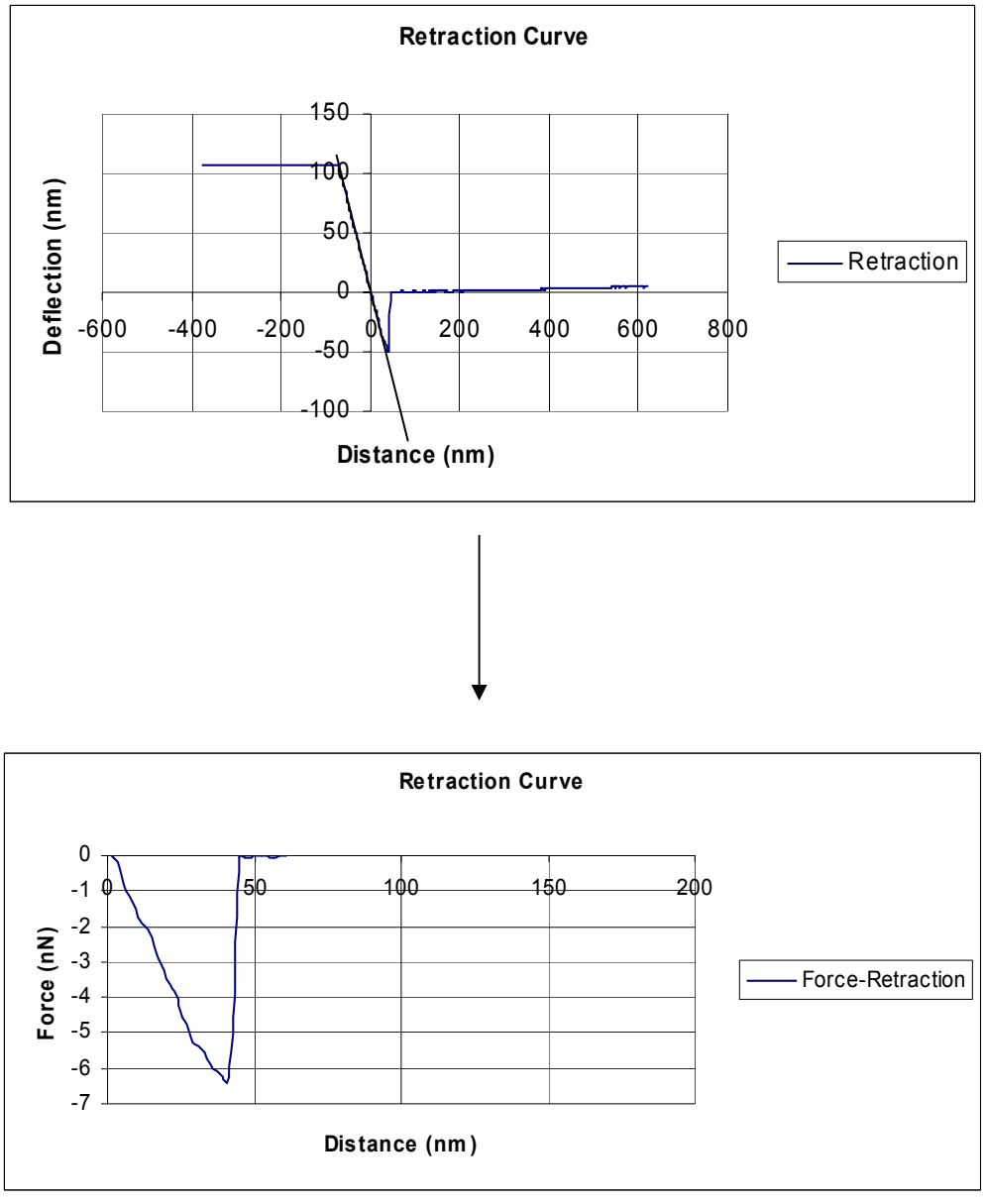

Figure 9(b)

The force curves were obtained on a silanized glass slide with silicon nitride tip under DI water.

The set of curves got for each force curve captured were analyzed by averaging the approach curves for all the different cells and the retraction data was plotted for all the cells on the same chart for comparison between cellulase treated and untreated retraction peaks.

4.0 Results and Discussion

The glass slides bonded with bacterial cells were placed under the atomic force microscope and force curves were captured on the bodies of the cells centered in the scan area. The approach and retraction curves captured on the cells were then regenerated as force-distance plots in excel. The curves were adjusted to correct for the force exerted by the cell by "zeroing" the force curves both on x and y axis. The average of the 4-5 approach curves captured on each untreated (U) cell for 5 cells was plotted and compared with that got for the average of the 4-5 approach curves captured on each cell for 5 enzyme-treated (ET) cells. Since the treatment process of the cells with enzyme included a number of centrifugation steps, a control experiment was performed in which the cells were grown to the same absorbance under similar conditions and kept untreated but were allowed to go through same number of centrifugation steps as was done for enzyme treated cells. 4-5 approach curves were averaged similarly for these untreated but centrifuged (UC) cells in a similar fashion as was done for the enzyme treated and untreated cells.

The retraction force curves were also analyzed and adjusted accordingly for cellulase treated, untreated and untreated but centrifuged cells to see to the change in magnitude of the attractive forces on the cell surfaces due to chemical (enzyme treatment) and physical (centrifugation) modifications.

4.1 Pseudomonas putida KT2442

The KT2442 cells were found using the AFM under DI water. Each cell was centered and imaged as shown in **Figure 10**. The cells were found to be in the range of 1-2 microns in size and 0.8-1.4 microns in height.

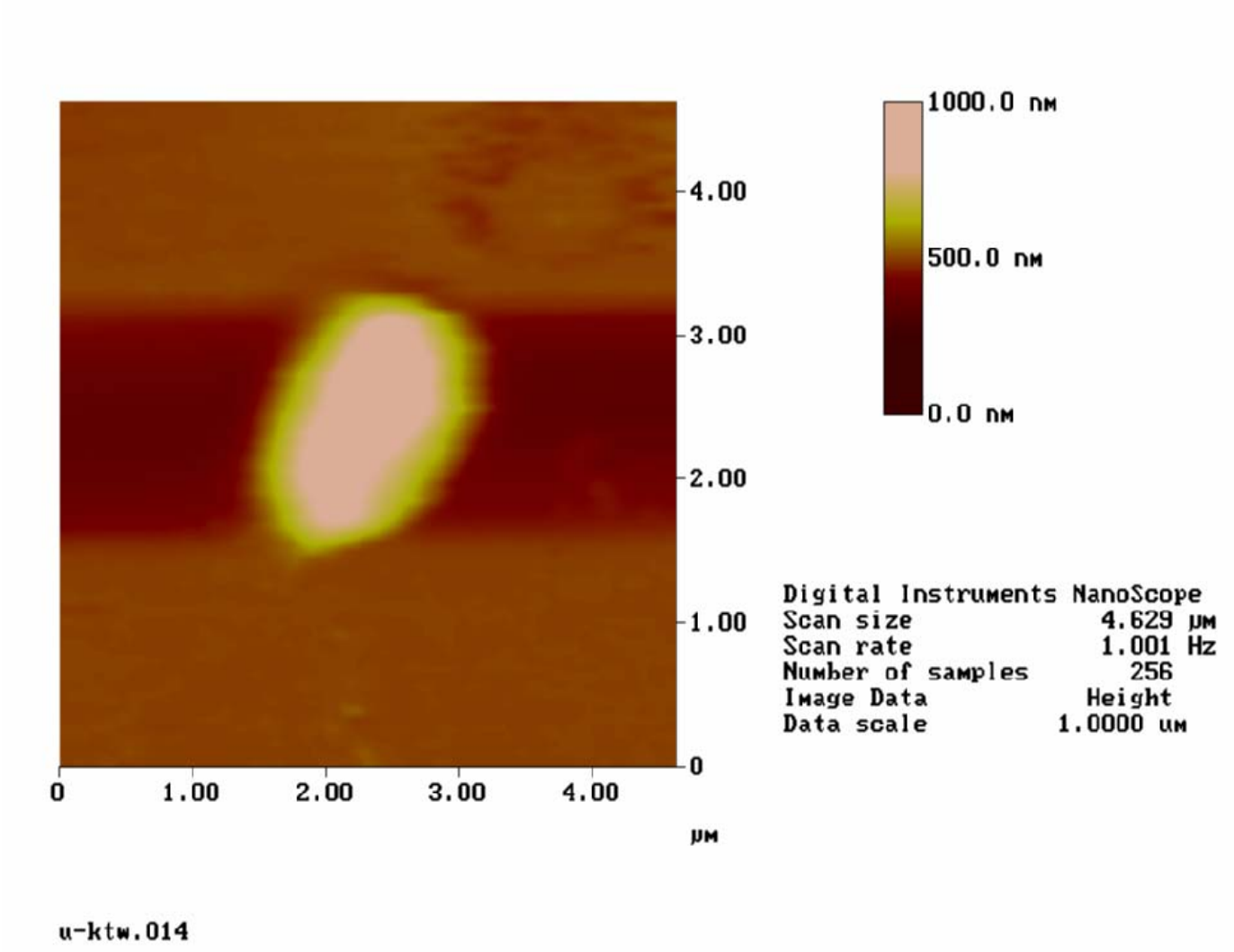

Figure 10: Image of a KT2442 cell, under water in tapping mode, brought to the center of the scan area, before capturing the force curve on the cell.

4.1.1 Approach curves for Pseudomonas putida before and after the cellulase treatment

The final approach curve upon averaging for the untreated KT2442 cells showed repulsion for the approaching silicon tip starting at several hundred nanometers away as is evident in **Figure 11**.

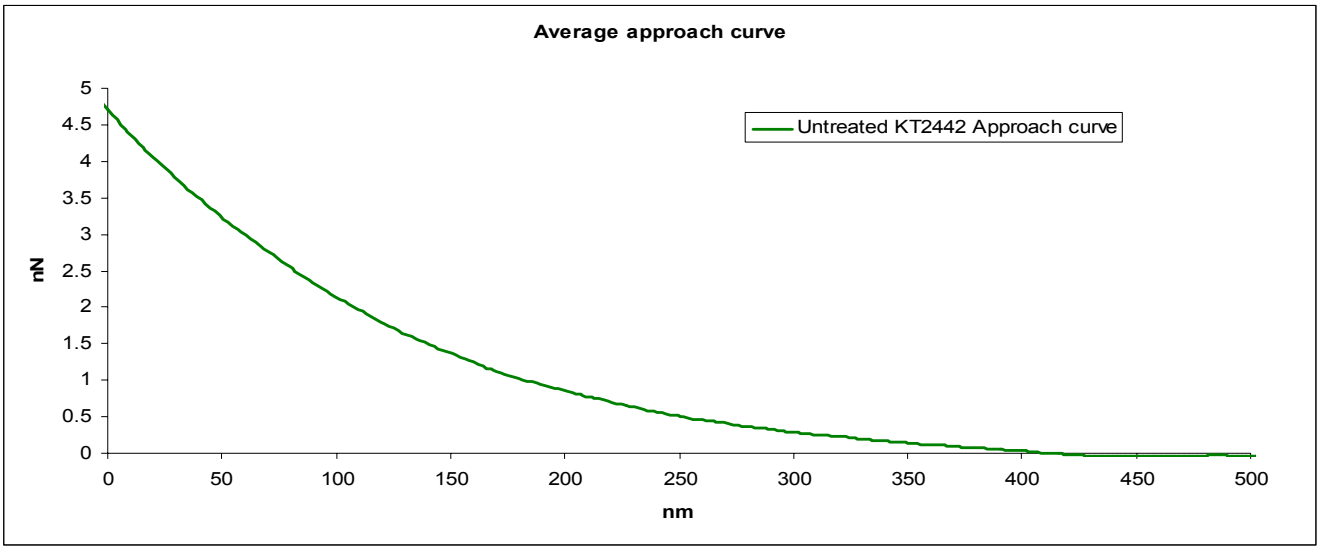

Figure 11: Approach curve obtained after averaging of 5 approach curves captured on each cell for 5 cells

Whereas for the cellulase treated cells the repulsion begins only a couple of hundred nanometers away from the cell surface and goes as high as 2.5 nN at the cell surface (**Figure 12**). Thus the treatment of the KT2442 cells results in a reduction of both the range and magnitude of the repulsive force at a given distance from the cell surface. The result could be due to the scission of the cellulose present on the cell surface or due to the attrition of the biopolymers present on the cell surface because of the centrifugation steps or due to the combined effect of the both.

The difference due to the treatment as depicted by force curves obtained using AFM is more evident in the comparison plot (**Figure 13**).

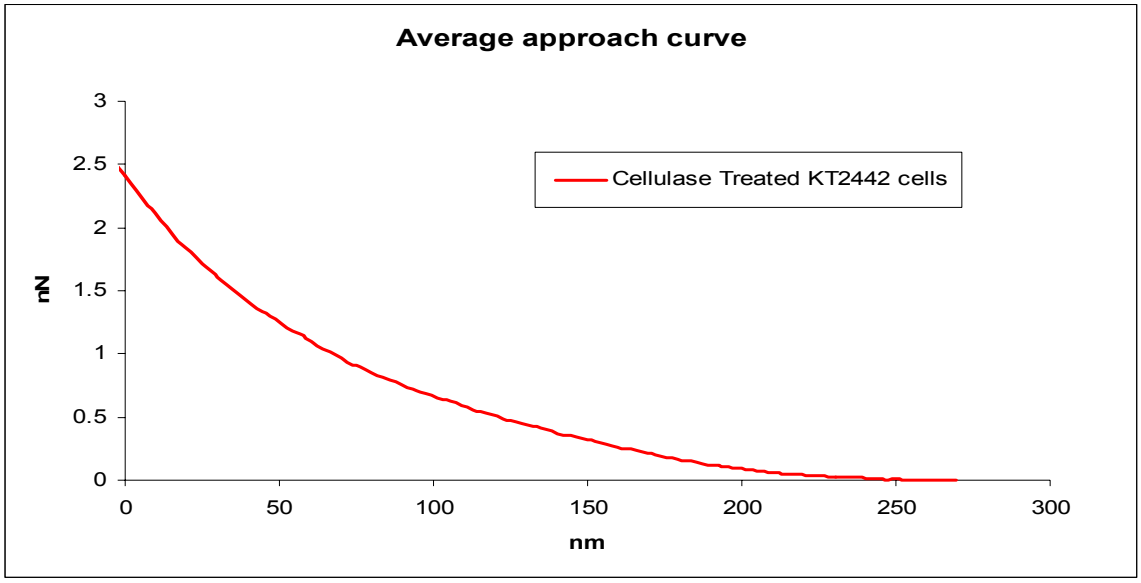

Figure 12: Approach curve obtained after averaging of 5 approach curves captured on each cell for 5 cells

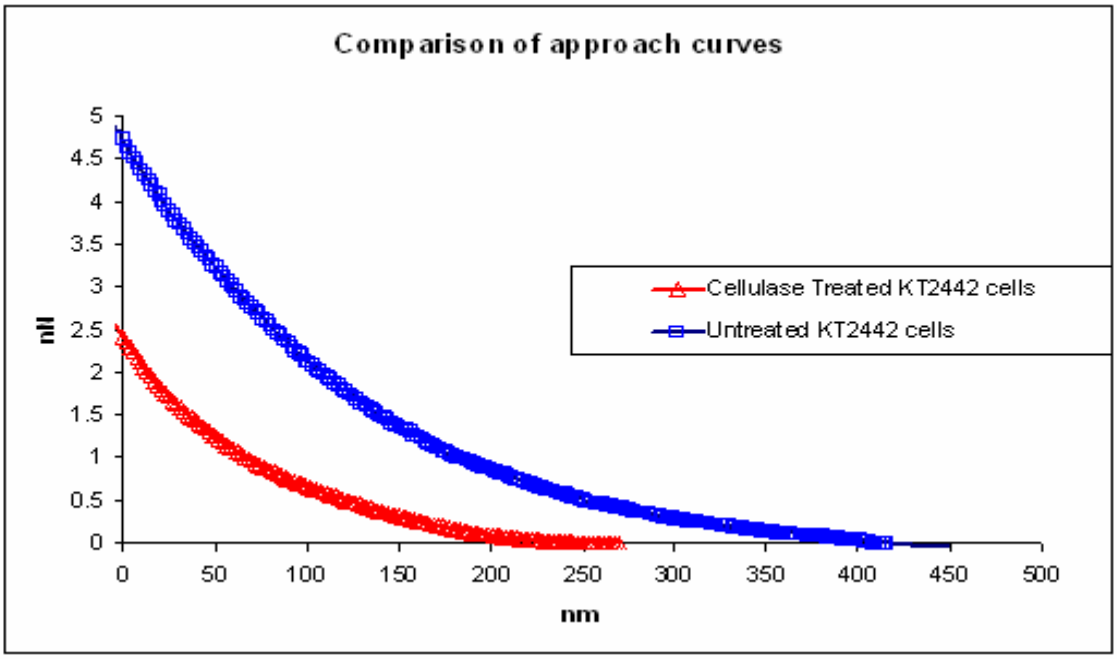

Figure 13: Approach curve obtained after averaging of 5 approach curves captured on each cell for 5 cells

A control experiment was performed on the untreated cells by treating the cells in the same fashion as was done for the cellulase treated except, actually treating the cells with cellulase. The control was performed to check the influence of centrifugation steps on the final results. The approach curve obtained for the control run by averaging 5 approach curves captured on each cell for 5 cells was almost same as obtained for the untreated cells (**Figure 14**).

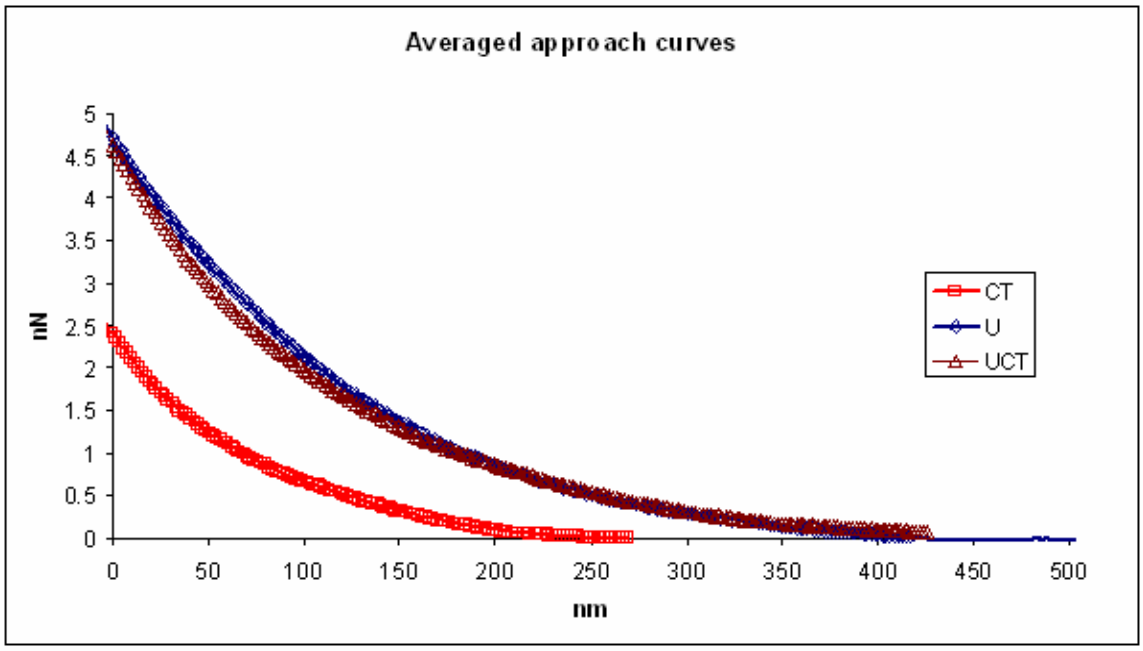

Figure 14: CT-Cellulase treated, U-Untreated, UC-Untreated but centrifuged (Control)

4.1.2 Steric Model

The approach force curves obtained for untreated, cellulase treated and control cells were fitted against the steric model assuming the repulsion was mainly due to the biopolymers extending from the cell surface since van der Waals and electrostatic forces are short range forces and can not extend to distances that we found in our case. The steric model applied to the force curves included two fitting parameters grafting density (m^{-2}) and polymer chain length (nm).

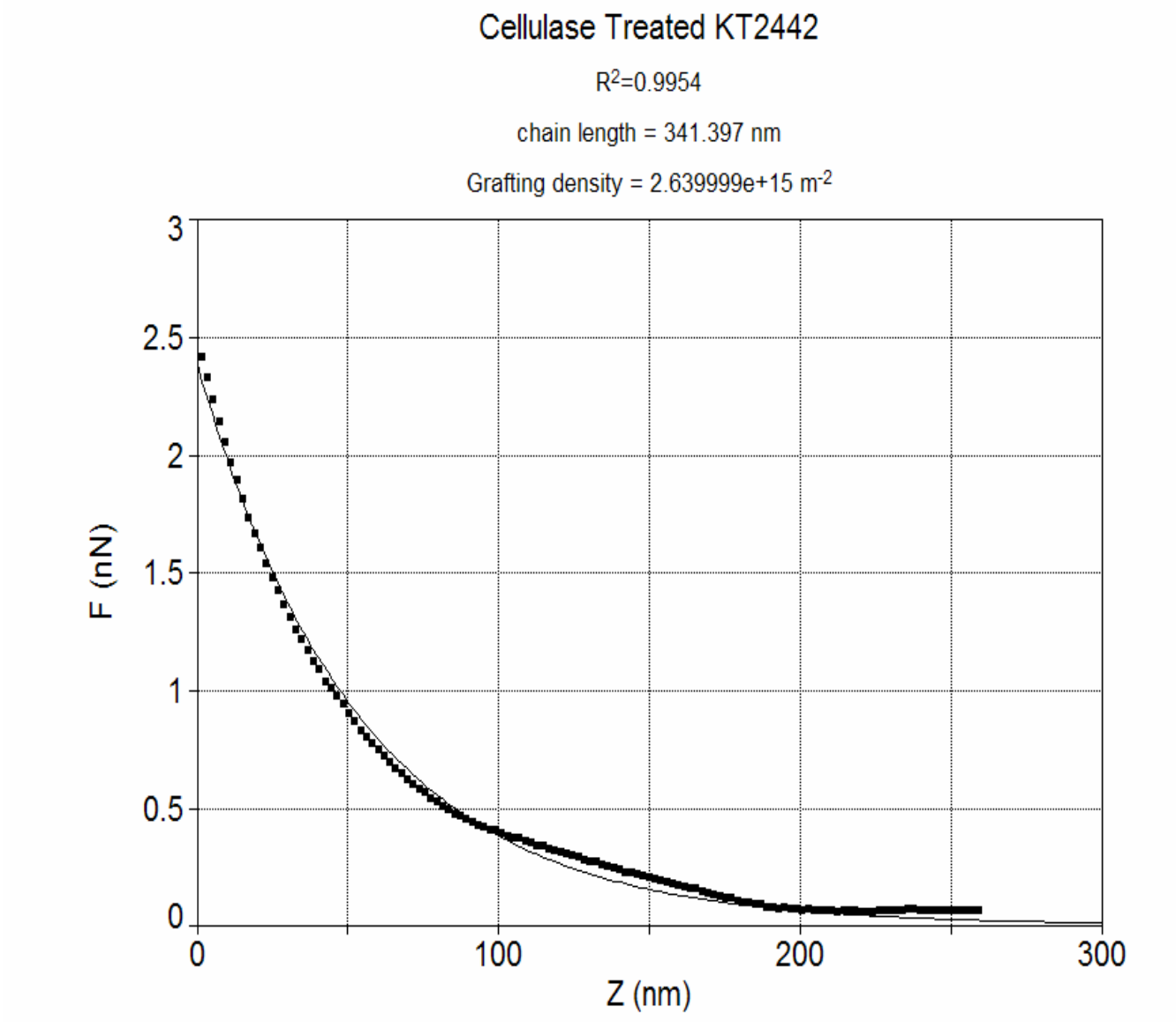

Figure 15: Cellulase treated fitting curve against steric model from TCWin

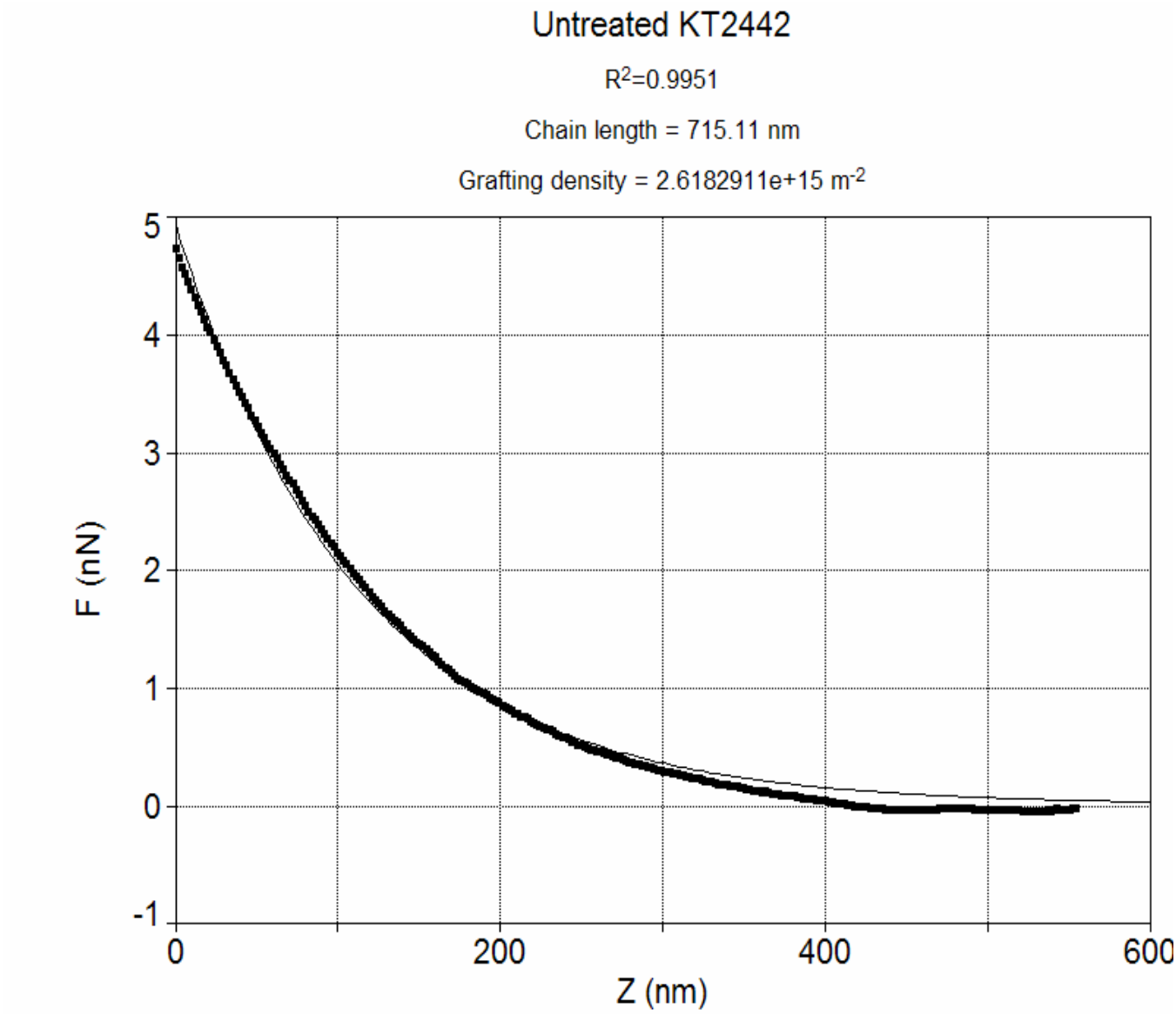

Figure 16: Untreated-centrifuged fitting curve against steric model from TCWin

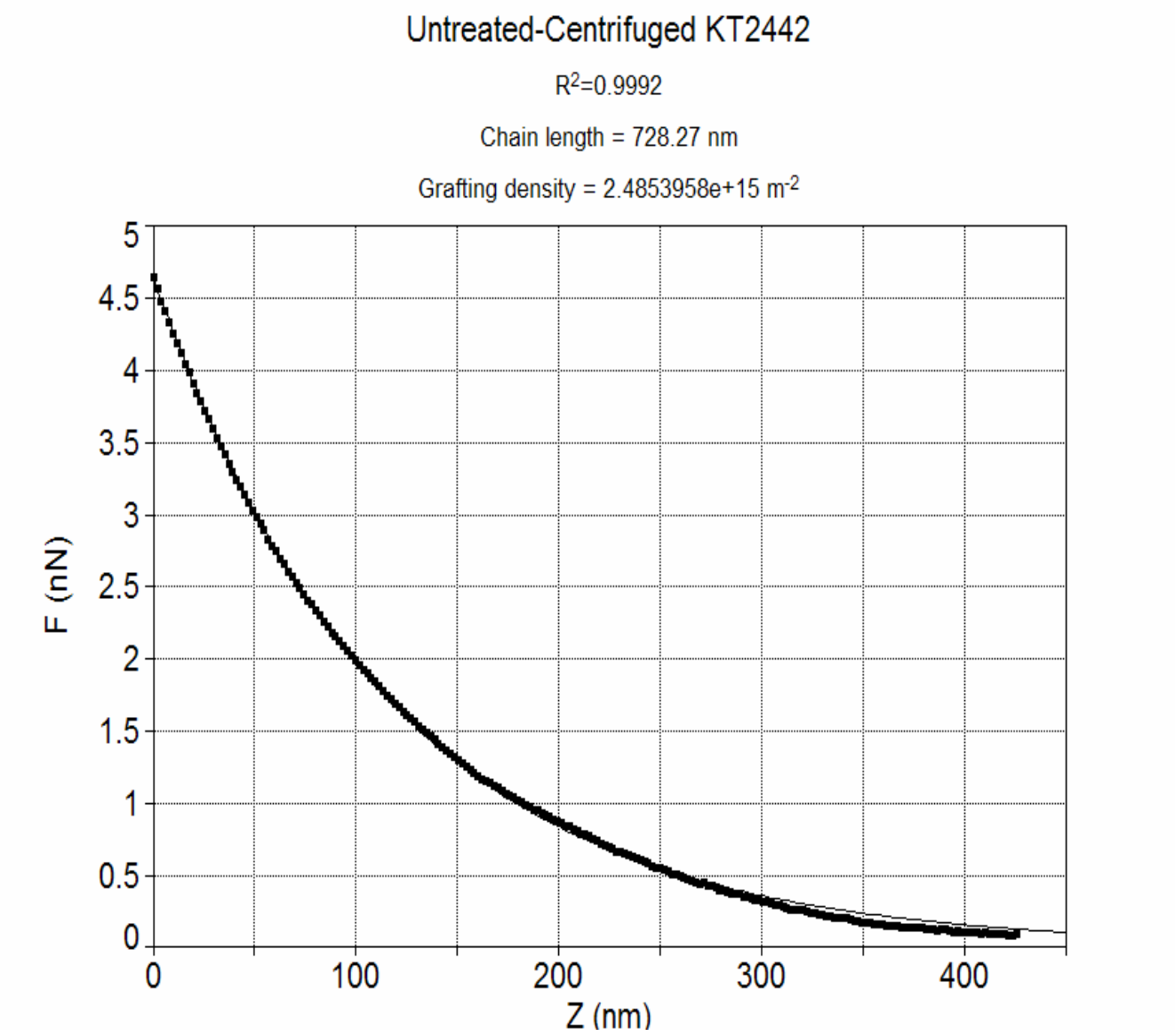

Figure 17: Untreated fitting curve against steric model from TCWin

	Cellulase Treated	**Untreated-Centrifuged**	**Untreated**
Regression	(99.49%)	(99.92%)	(99.51%)
Chain length (nm)	341.39	728.27	715.11
Grafting density (m^{-2})	2.64e+15	2.48e+15	2.61e+15

Table # 3: The chain length appears to be shortened for the biopolymers present on the cell surface after the cellulase treatment, as predicted by the steric model.

The fitting of the approach force curves with the steric model for each of the three cases allows for quantifying the results in terms of polymer brush length and grafting density (**Table # 3**). The grafting density of the polymers present on the cell surface remained almost the same with and without the cellulase treatment whereas the length of the brush decreased after the cellulase treatment. The chain length and grafting density for the untreated-centrifuged cells were found to be close to those for untreated cells indicating no contribution of the centrifugation steps, towards decreased repulsion upon cellulase treatment, quantitatively.

4.1.3 Carbohydrate Assay

The assay was run to check if any biopolymers came off during the centrifugation process which might not be detected with the atomic force microscopy experiments. The experiment performed included the anthrone test on 1 ml of the supernatant sample from each post-centrifugation step.

Anthrone assay:

1 ml of the bacterial sample (diluted/undiluted) was mixed with 1 ml of 100% HCl acid.

0.1 ml of 90% formic acid was added to the above solution.

8 ml of Anthrone solution (Anthrone 20mg in 80% H2SO4) was slowly poured into the 25cm glass tube containing the sample solution.

The tubes containing samples in different dilutions were then kept in hot water bath for 12 minutes.

Degree of change in color of the sample solutions indicated the amount of sugar present in different dilutions. The absorbance was recorded for all the samples and compared with the Anthrone solution (as blank) and with water (as blank) to check for the presence of sugars in all the samples.

Absorbance of the supernatant solution at two different dilutions 1:1 and 1:10 were measured @ a wavelength of 600nm after each centrifugation step (**Table # 4**). Absorbance of the Anthrone treated diluted samples was measured @ 630nm (**Table # 5**).

	Untreated cells (Abs @ 630 nm)	**Untreated-Centrifuged cells (Abs @ 630 nm)**	**Cellulase treated cells (Abs @ 630 nm)**
1st centrifugation	0.021	0.025	0.020
2nd centrifugation	0.030	0.025	0.021
3rd centrifugation	-	0.014	0.028
4th centrifugation	-	0.014	0.010
5th centrifugation	-	0.010	0.017

Table # 4: Absorbance measured for the supernatant samples after each centrifugation step for Untreated, cellulase treated and Untreated-centrifuged cells.

The third centrifugation step shows an increase in the absorbance of the cellulase treated supernatant indicating removal of biopolymers from the cell surface in the cellulase treatment step performed just prior to the third centrifugation. Whereas for the Untreated-centrifuged cells the absorbance is very low indicating that at this stage the biopolymers are not coming off of the cell surface anymore. This argument is well supported by the results from the Anthrone test for different dilutions of the supernatant samples gave similar results (**Table # 5**).

The absorbance was measured relative to the Anthrone sample @ 630nm. The results showed the presence of carbohydrate in the supernatant obtained from the centrifugation step right after the cellulase treatment step, whereas no carbohydrate was detected with the Anthrone assay in the supernatant sample for Untreated-centrifuged cells. Also for the untreated cells the supernatant did not have a lot of carbohydrate released into it. The small amount of carbohydrate released into the

supernatant after 2nd centrifugation of the untreated cells can be explained as removal of loosely bound biopolymers due to the centrifugation action. But after 2-3 centrifugations the biopolymers present on the cell surface are only those which are tightly bound to the surface and could only come off with the help of some specific enzyme activity.

Blank used = Anthrone

Dilution	Sample (1ml)	Absorbance @ 630nm
1-1	Untreated supernatant-2	0.024
1-10	Untreated supernatant-2	-
1-1	UC-supernatant-3	-
1-10	UC-supernatant-3	-
1-1	CT-supernatant-3	0.152
1-10	CT-supernatant-3	0.085

Table # 5: Anthrone test results for i) Untreated cells at 2nd centrifugation, ii) Untreated-centrifuged cells at 3rd centrifugation and iii) Cellulase treated at 3rd centrifugation

4.1.4 Retraction curves for Pseudomonas putida KT2442 cells

The retraction force curves were zeroed like the approach curves (**Figure 18**). The magnitude of the peaks in the zeroed-retraction force curve was plotted against the distance at which the pull occurs (**Figure 19**). The adhesion peak is represented by the inverted peak in **Figure 18** indicating the

force (Blue arrow) with which the tip is pulled back by the surface polymers. The distance at which the polymer-tip bond breaks is represented by the red arrow in **Figure 18**.

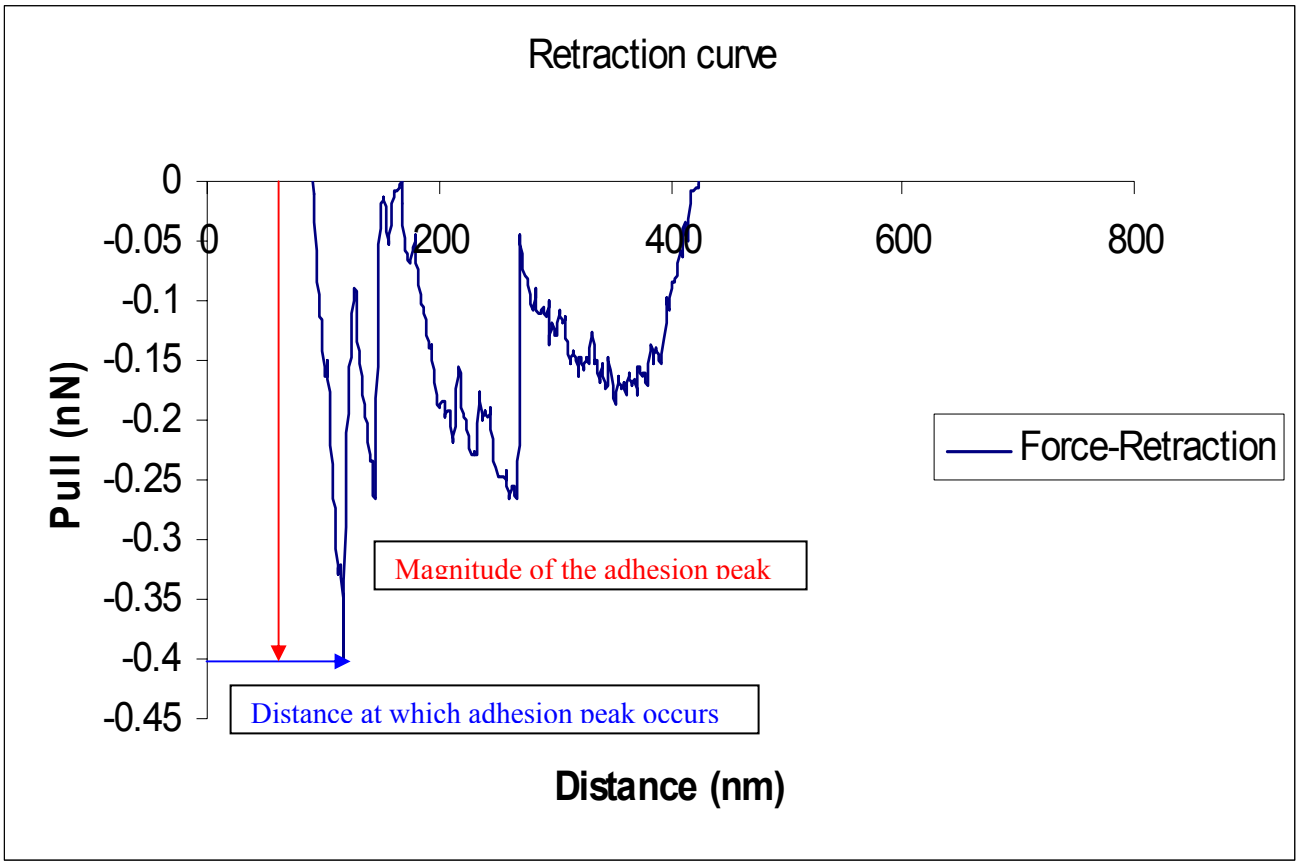

Figure 18: Representative example of a retraction curve for cellulase treated KT2442 cells.

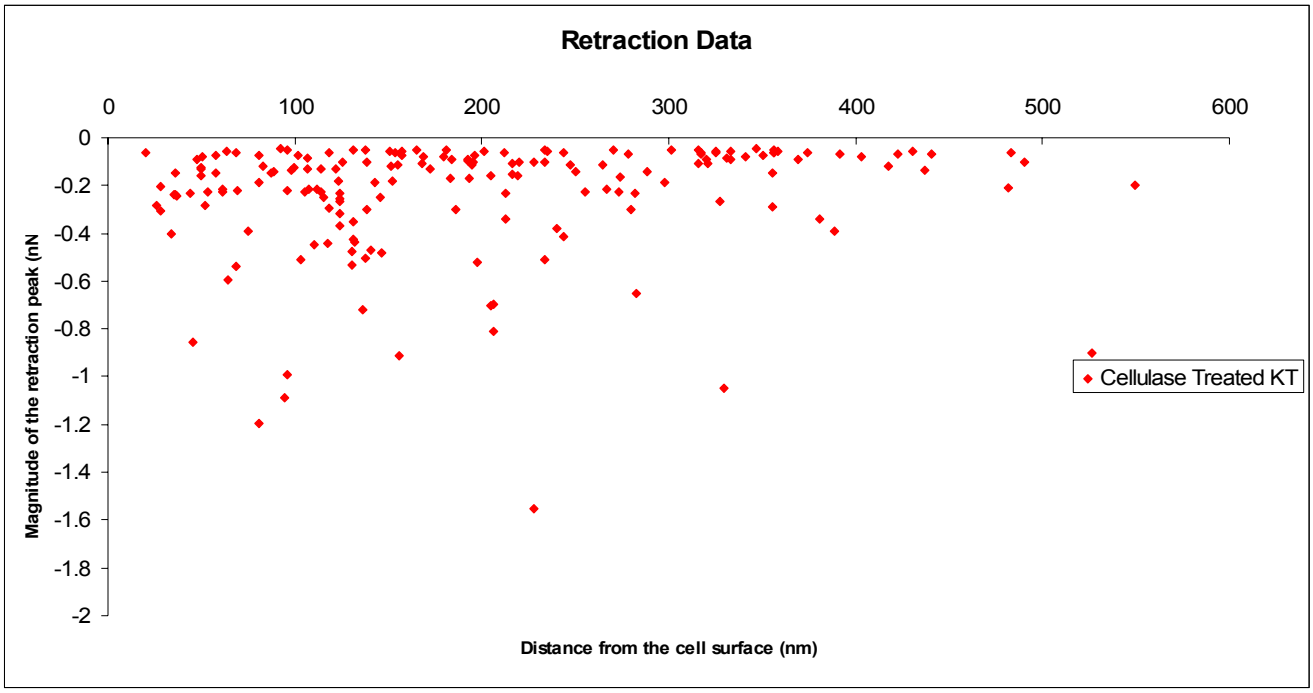

Figure 19: Plot of all the adhesion peaks captured for all the cellulase treated cells

The retraction data for the untreated KT2442 were plotted as was done for the cellulase treated cells (**Figure 20**).

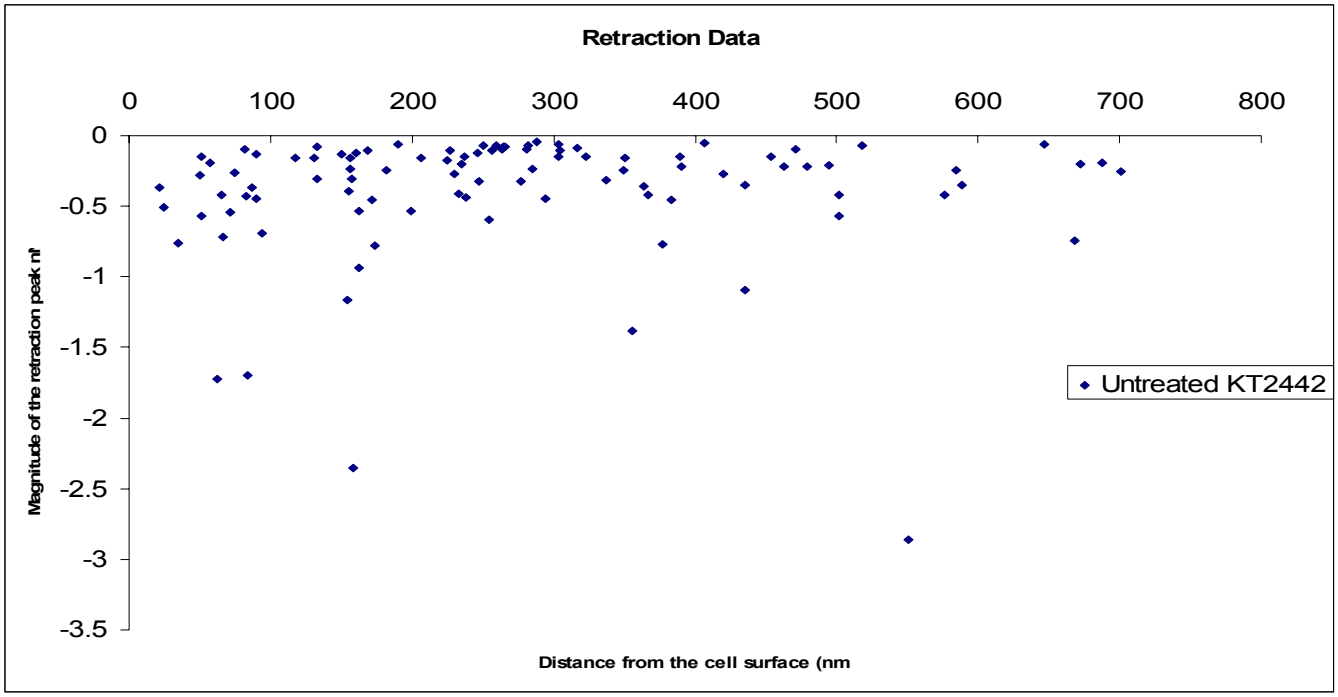

Figure 20: Plot of all the adhesion peaks captured for all the cellulase treated cells

Upon comparison between the untreated and cellulase treated KT2442 cells on the retraction basis the cellulase treated cells were found to have slightly reduced forces of attraction and extending to shorter distances than for the untreated cells (**Figure 21**). This indicates that the presence of cellulose on the KT2442 cell surface made it stickier and the cells should have a lower tendency to stick to a surface after the removal of cellulose from their surface.

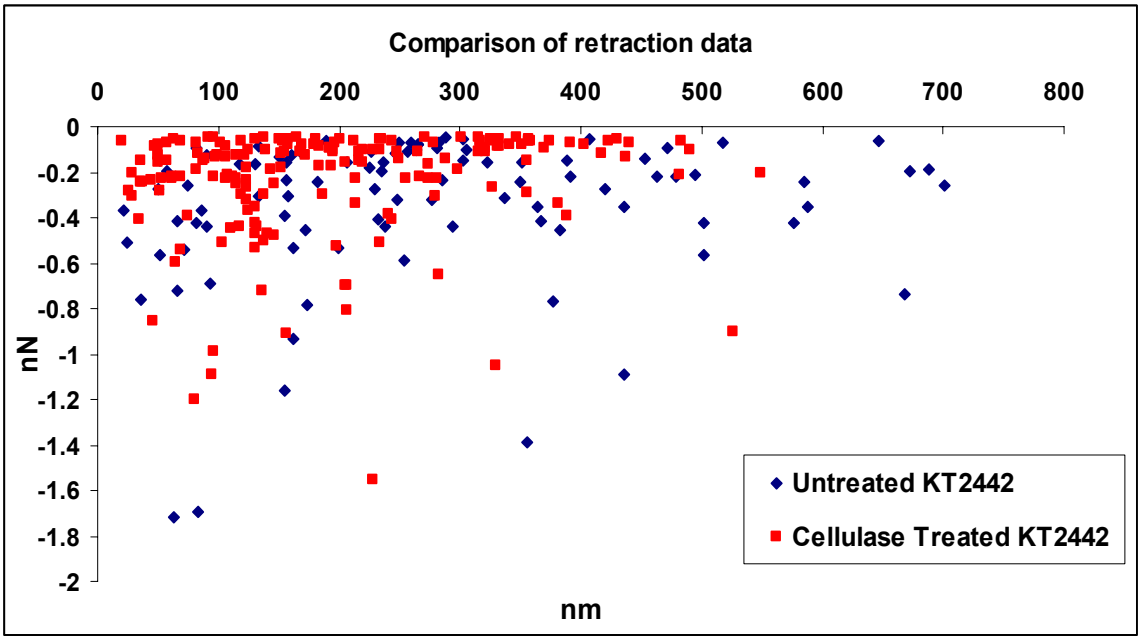

Figure 21: Comparison of retraction data between untreated and cellulase treated KT2442 cells

Further to verify the absence of any role played by the centrifugation steps, the retraction curves for the untreated cells were compared with those of the untreated-centrifuged cells. The data points ranged to the same magnitude of forces and to the same extent from the cell surface for both the untreated and untreated-centrifuged cells (**Figure 22**).

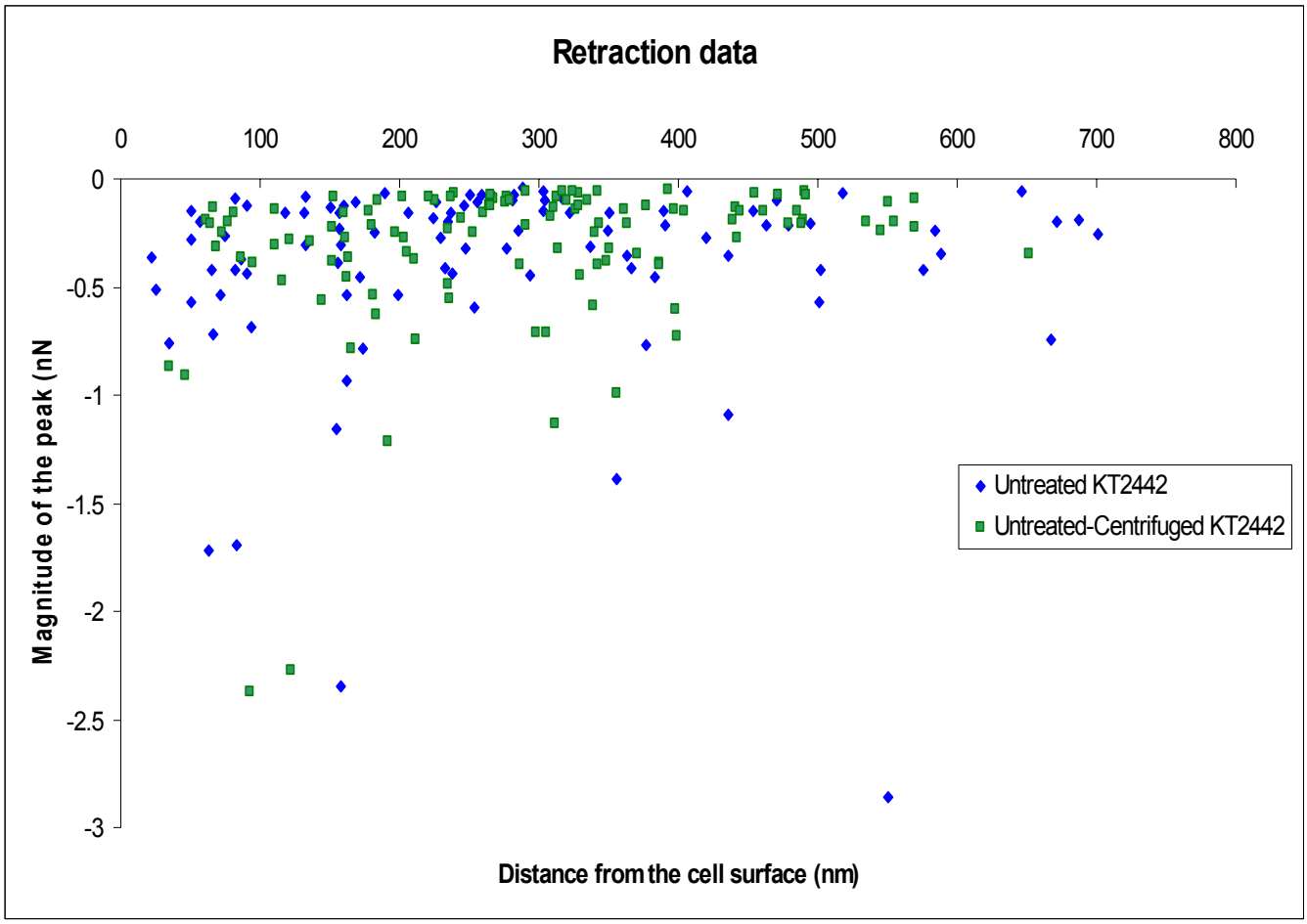

Figure 22: Comparison between Untreated and Untreated-Centrifuged (control) KT2442 retraction data.

The results based on the retraction curves were compared on the basis of normalized number of instances of a certain magnitude of pull experienced by the AFM tip (**Figure 23**), and on the basis of the number of pull instances in a certain range of distance (**Figure 24**), for the cellulase treated and untreated KT2442 cells.

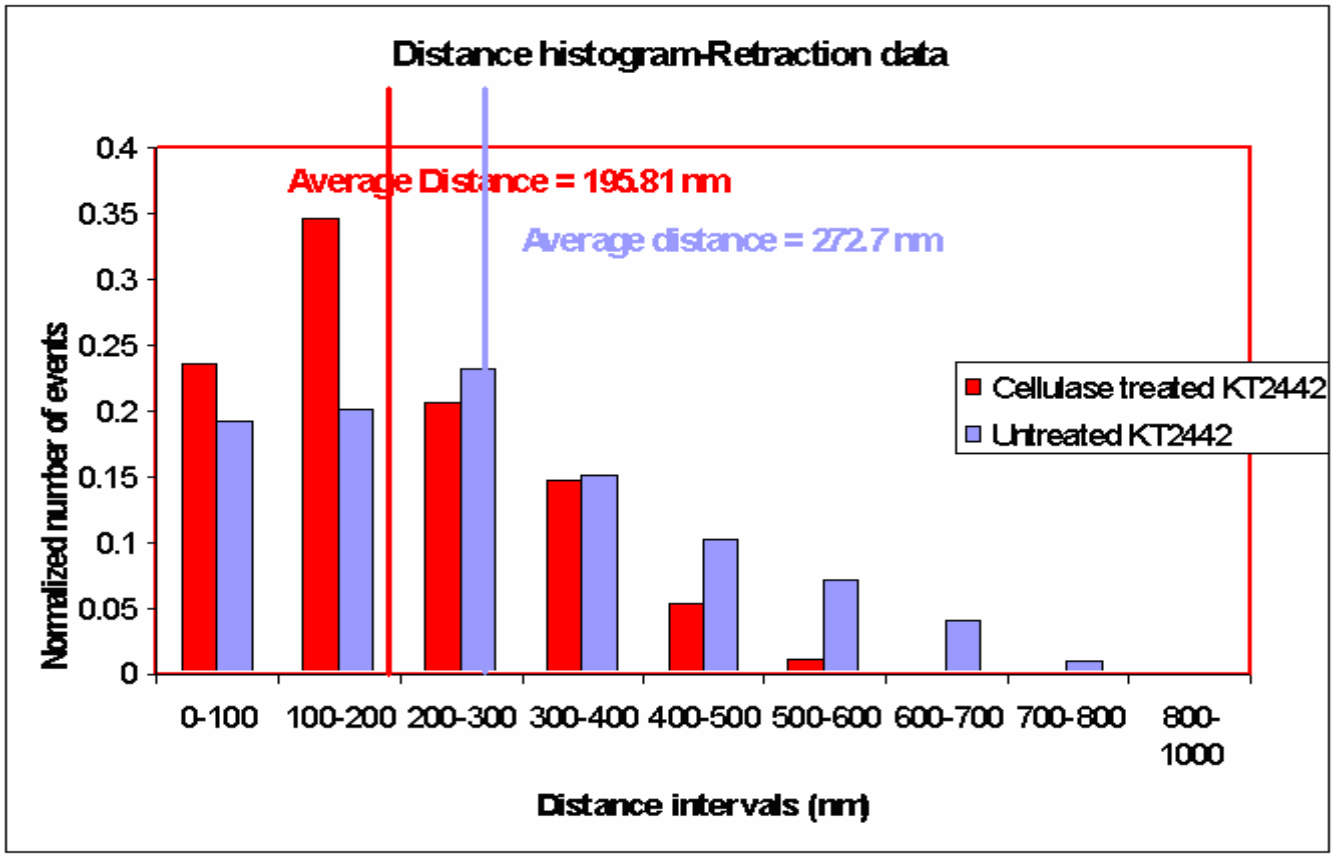

Figure 23: Comparison of normalized number of events occurring in a certain distance range for each case

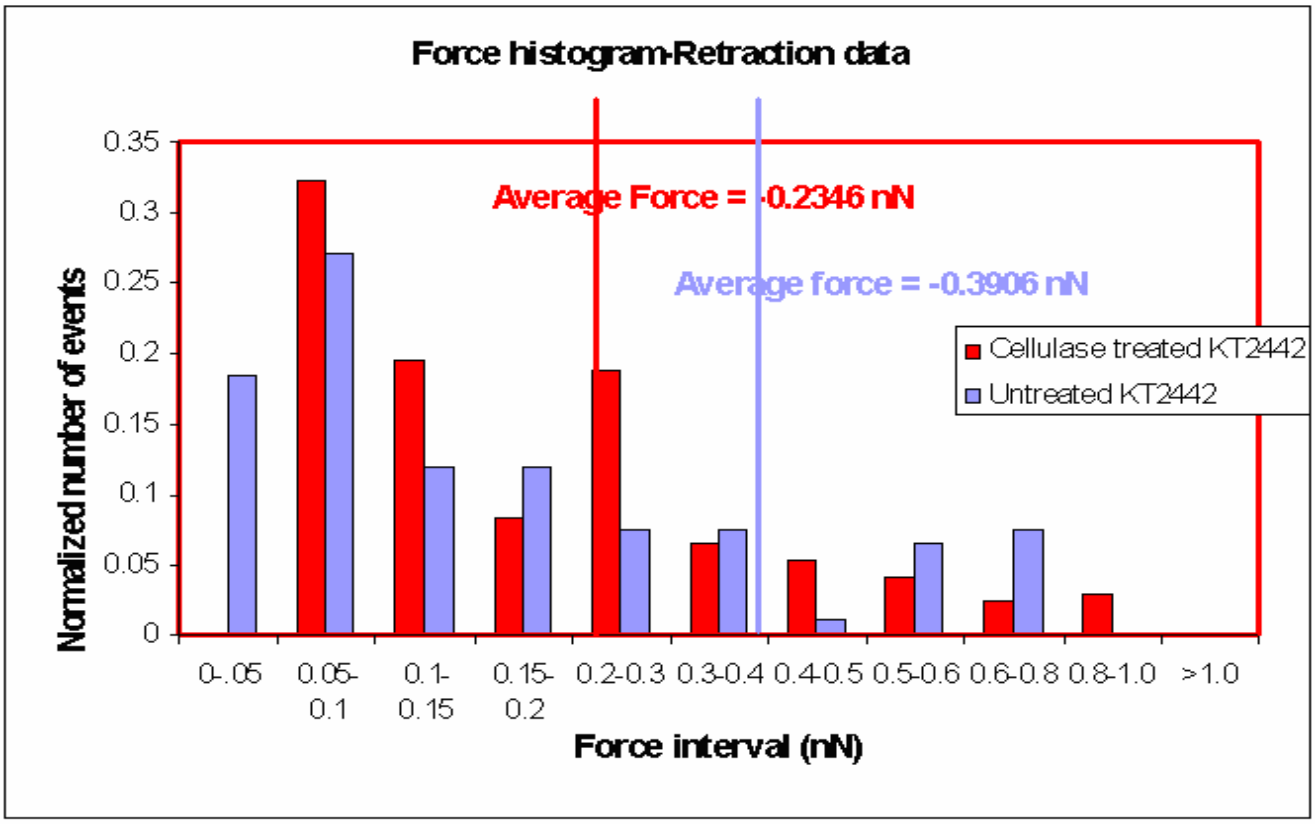

Figure 24: Comparison of normalized number of events occurring in a certain force range for each case

Overall the force of repulsion and attraction both decreased after the enzyme treatment for the KT2442 cells accompanied with a decrease in the length of the biopolymer chains present on the cell surface.

4.2 Leuconostoc mesenteroides NIRC1542

The NIRC1542 cells were found using the AFM under DI water. Each cell was centered and imaged as shown in **Figure 25**. The cells were found to be in the range of 0.5-1.0 microns in size and 0.6-1.2 microns in height.

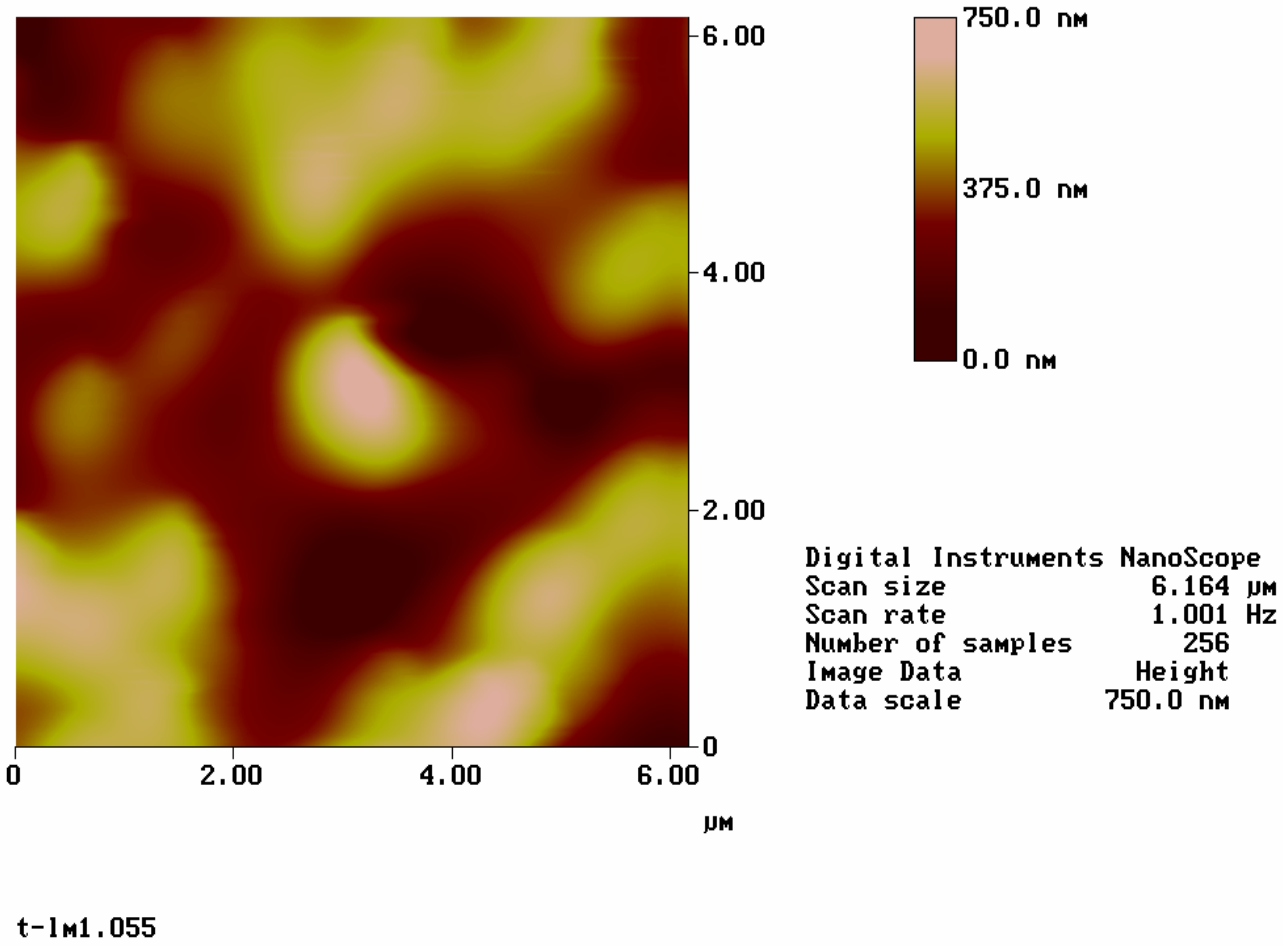

Figure 25: Image of a NIRC1542 cell brought to the center of the scan area, before capturing the force curve on the cell.

4.2.1 Approach curves for Leuconostoc mesenteroides before and after the dextranase treatment

Further the results obtained for the *Leuconostoc mesenteroides* NIRC1542 cells were analyzed. After doing AFM experiments on the untreated and dextranase treated NIRC1542 cells in the same way as were done for the KT2442 cells, the captured force curves were averaged and compared. **Figure 17** shows both the averaged approach curves for the untreated NIRC1542 cells.

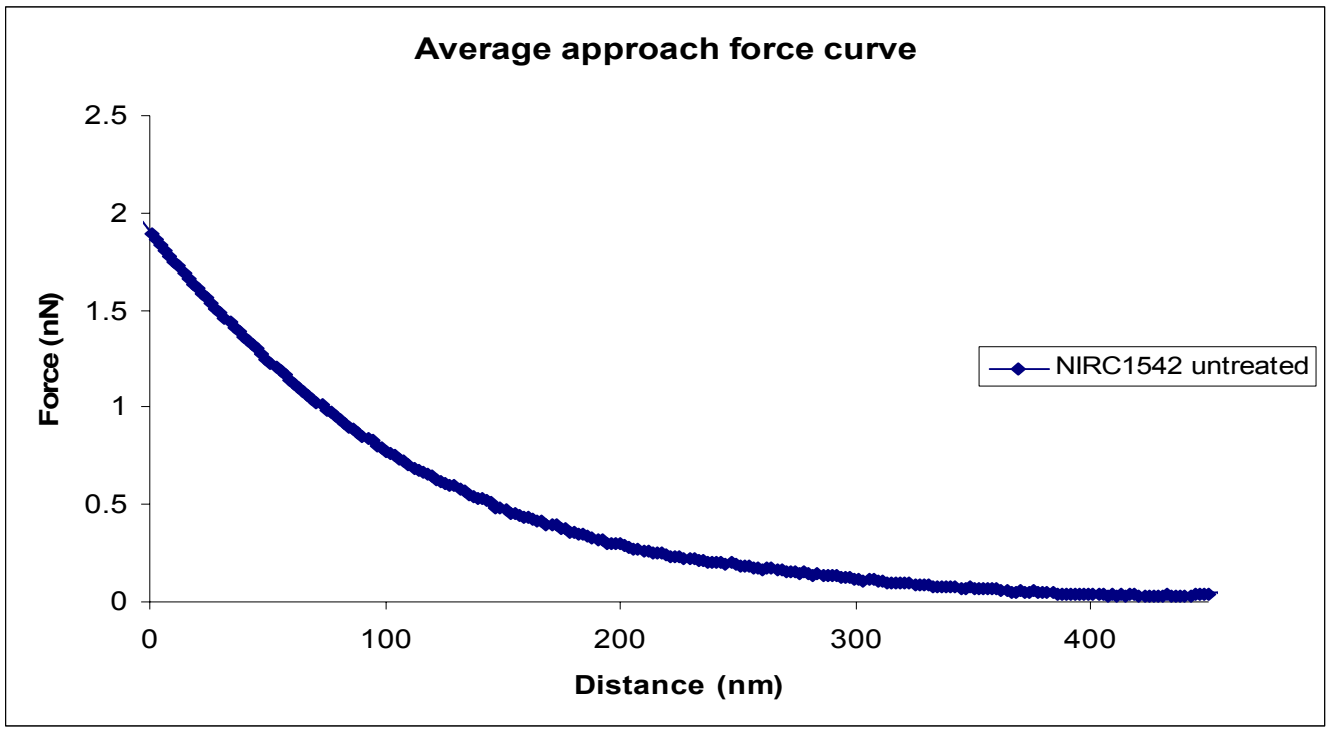

Figure 26: Average approach force curve for the untreated LM NIRC1542 cells under DI water

From the same batch of the grown NIRC1542 cells, same amount of cells were treated with dextranase and the cells were bonded to the clean glass slides. The force curves captured for the dextranase treated NIRC1542 cells were regenerated and zeroed in the excel sheets (**Figure 26**). The approach force curves were averaged and compared with the average of the approach curves obtained for the untreated cells (**Figure 27**).

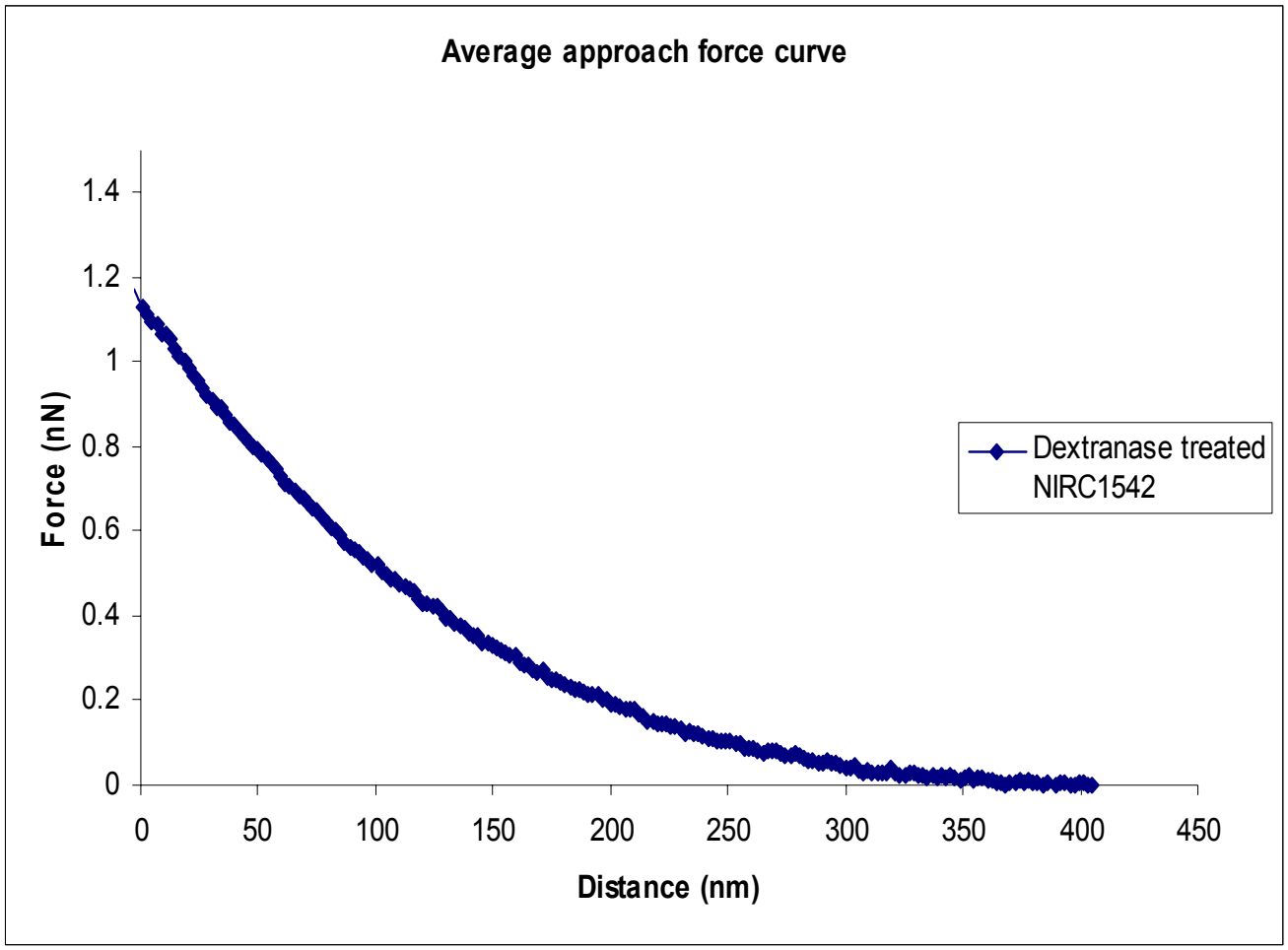

Figure 27: Averaged approach force curve for the dextranase treated LM NIRC1542 cells

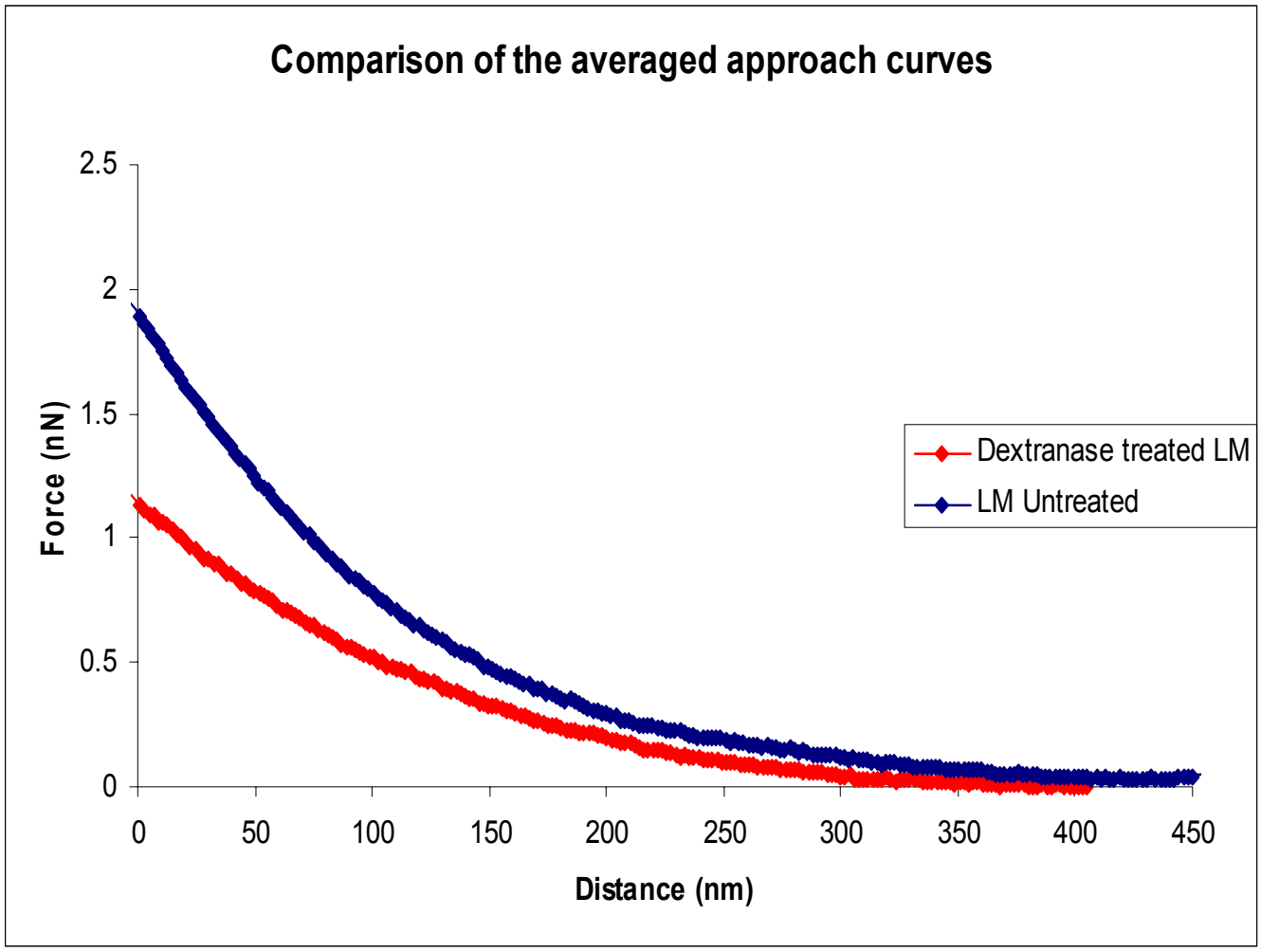

Figure 28: Comparison of the averaged approach force curves of dextranase treated (red) and untreated (blue) NIRC1542 cells. Dextranase treated cells show lower repulsion compared to the untreated cells as the silicon tip approaches the cell surface.

Chain length and grafting density parameters, for the treated and untreated set of cells, were deduced as upon fitting these approach force curves to the steric model using TCWin.

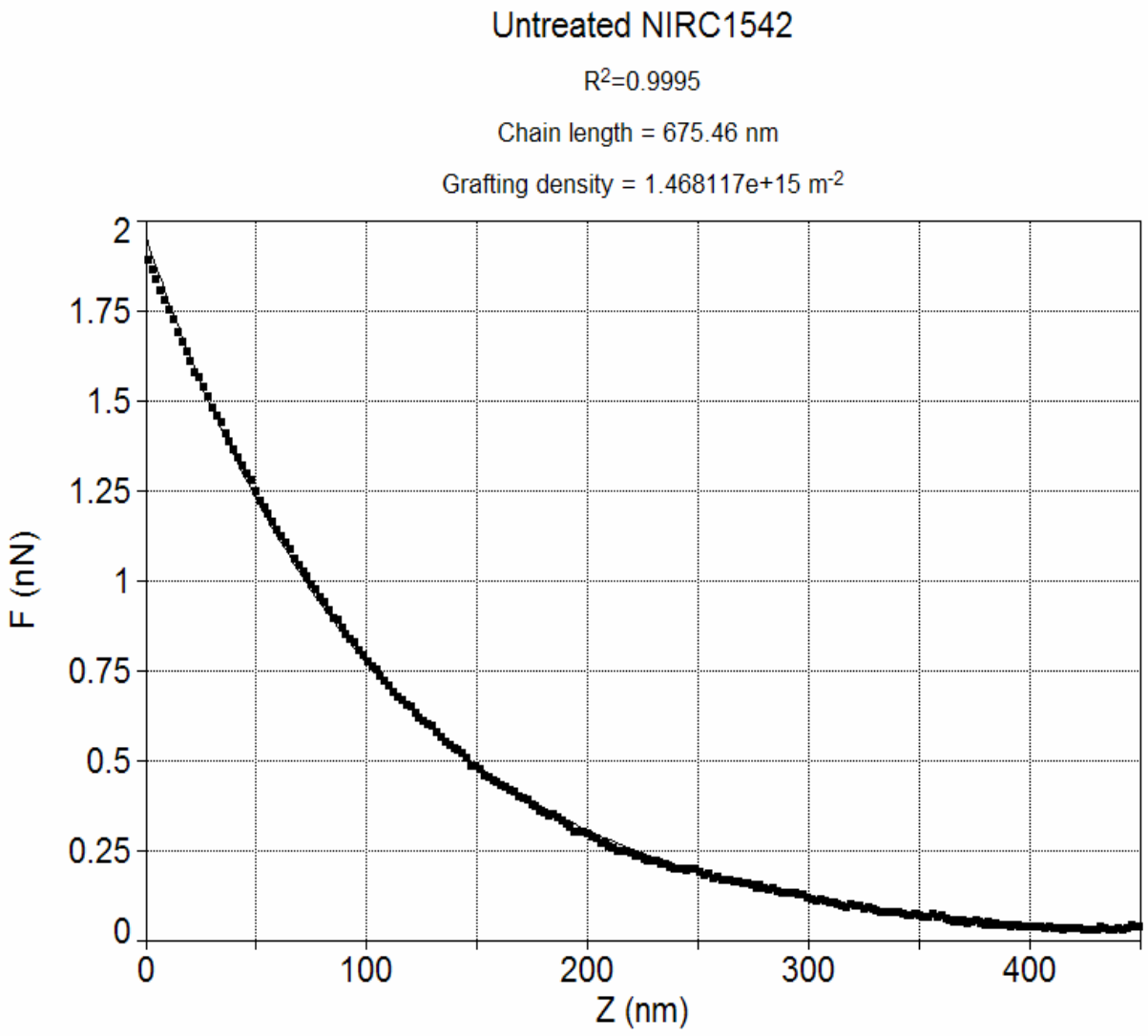

Figure 29: Averaged approach curve for the untreated NIRC1542 fitted to the steric model

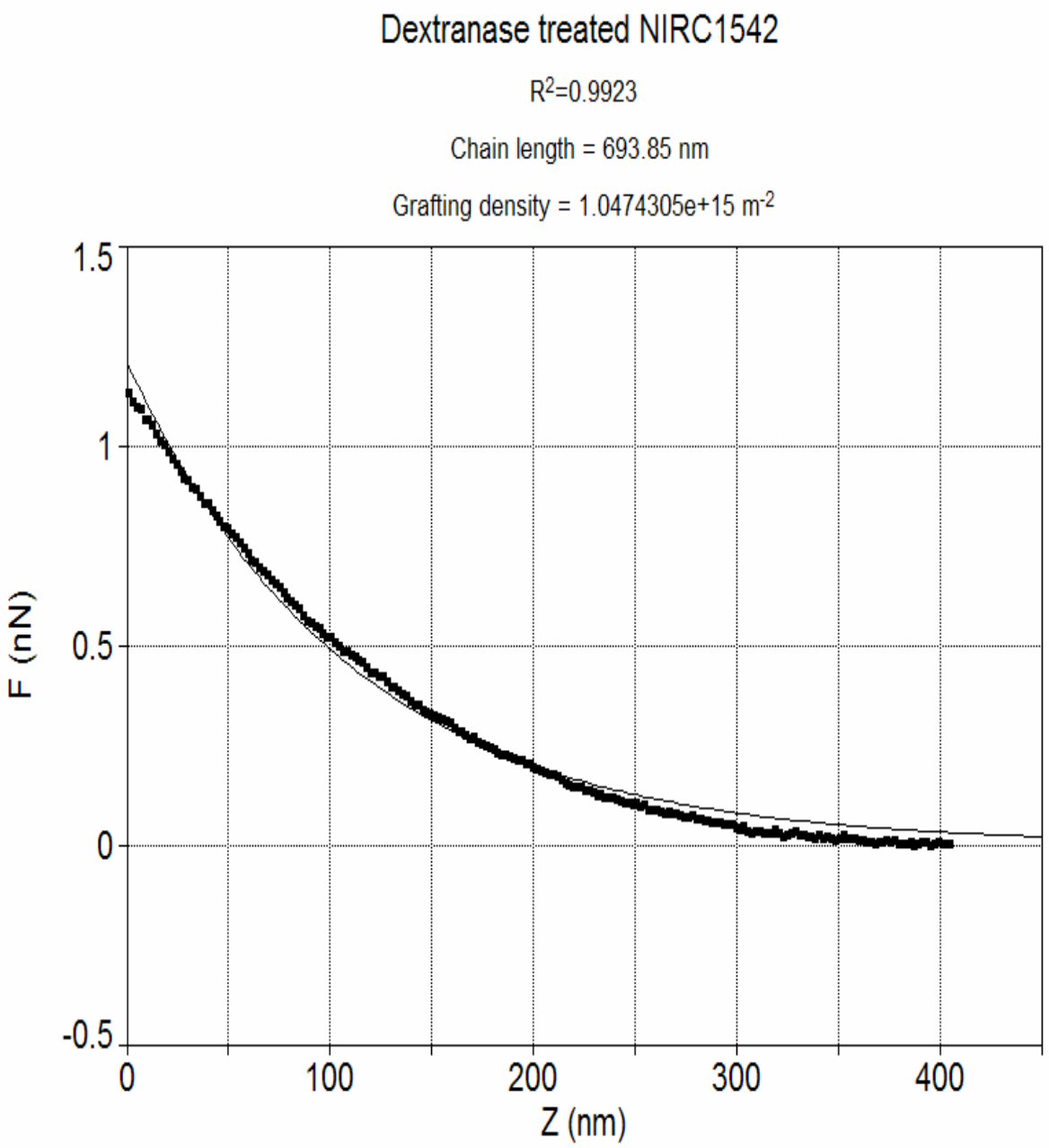

Figure 30: Averaged approach curve for the dextranase treated NIRC1542 fitted to the steric model

	Dextranase-treated NIRC1542	**Untreated NIRC1542**
Regression	(99.23%)	(99.92%)
Chain length (nm)	693.85	675.46
Grafting density (m^{-2})	1.0474305e+15	1.468117e+15

Table # 6 The grafting density appears to be reduced for the biopolymers present on the cell surface, where as the chain length remains almost the same after the dextranase treatment, as calculated by the steric model.

The fitting of the approach force curves with the steric model allows for quantifying the results in terms of approximate chain length and grafting density (**Table # 6**). The grafting density of the polymers present on the cell surface appeared to decrease after the dextranase treatment while the brush layer of the chain remained the same after the treatment.

4.2.2 Retraction curves for Leuconostoc mesenteroides NIRC1542 cells

The retraction force curves were zeroed like the approach curves truncating the effect of the body of the cell on the force curve. The magnitude of the peaks in the zeroed-retraction force curve was plotted against the distance at which the pull occurs for all the peaks.

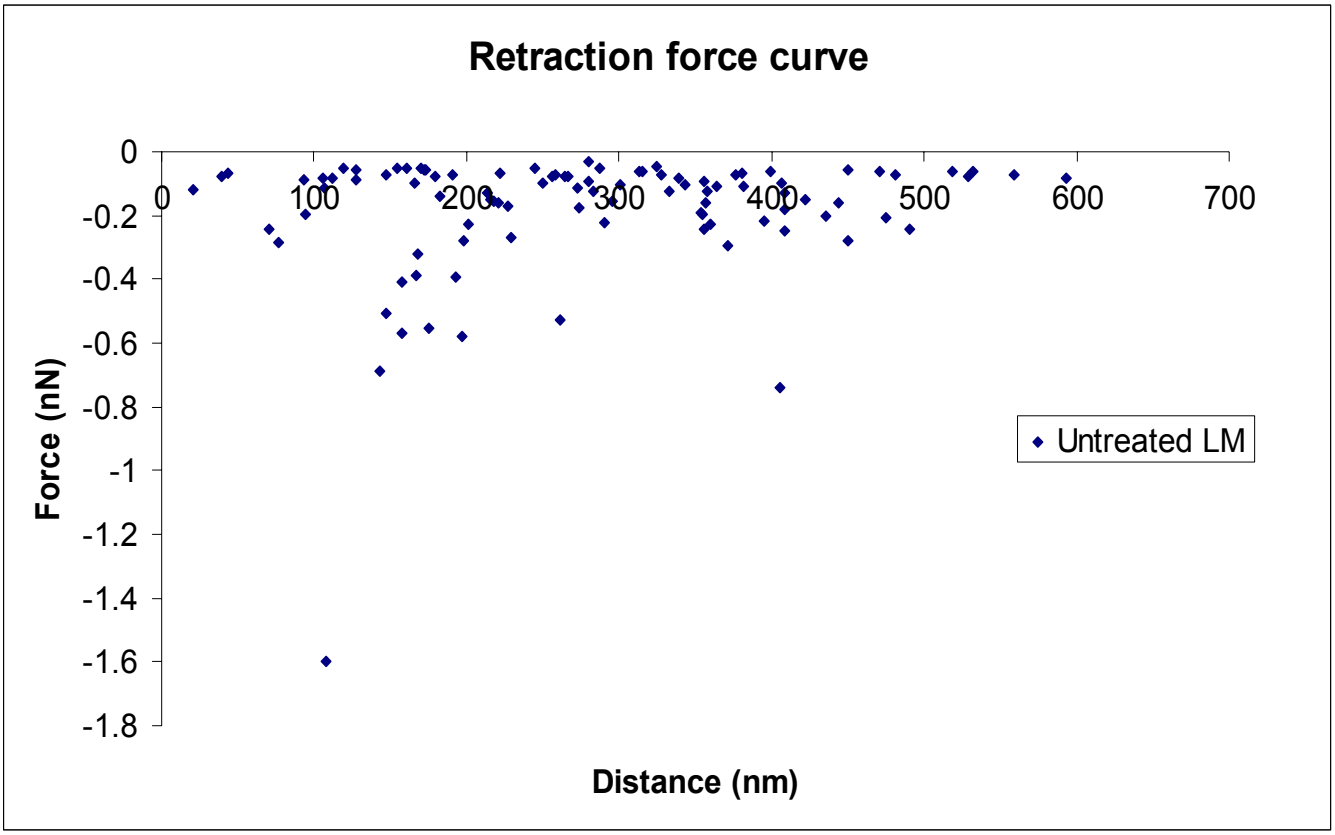

Figure 31: Retraction data for all the untreated NIRC1542 cells captured

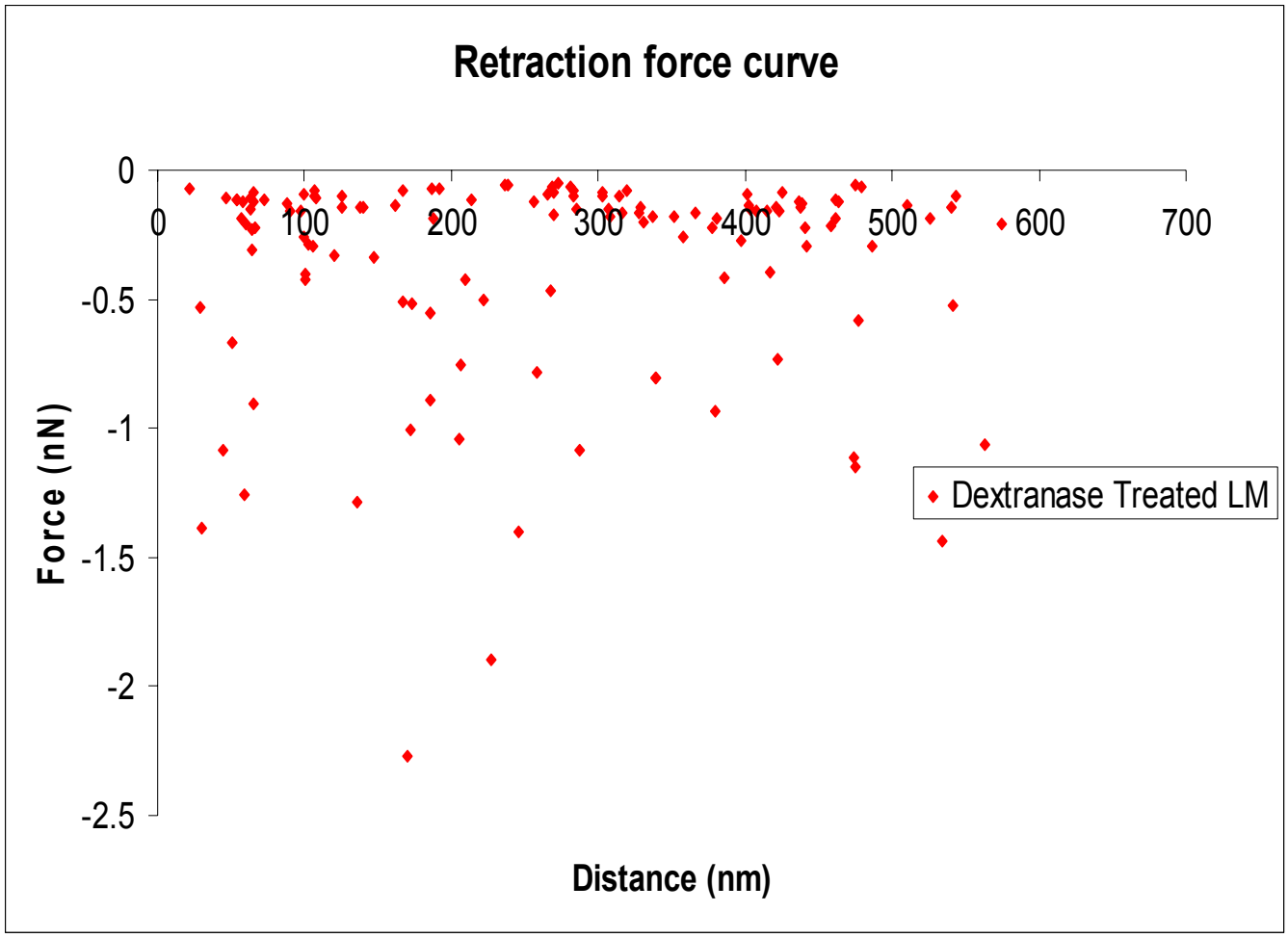

Figure 32: Retraction data for all the dextranase treated NIRC1542 cells

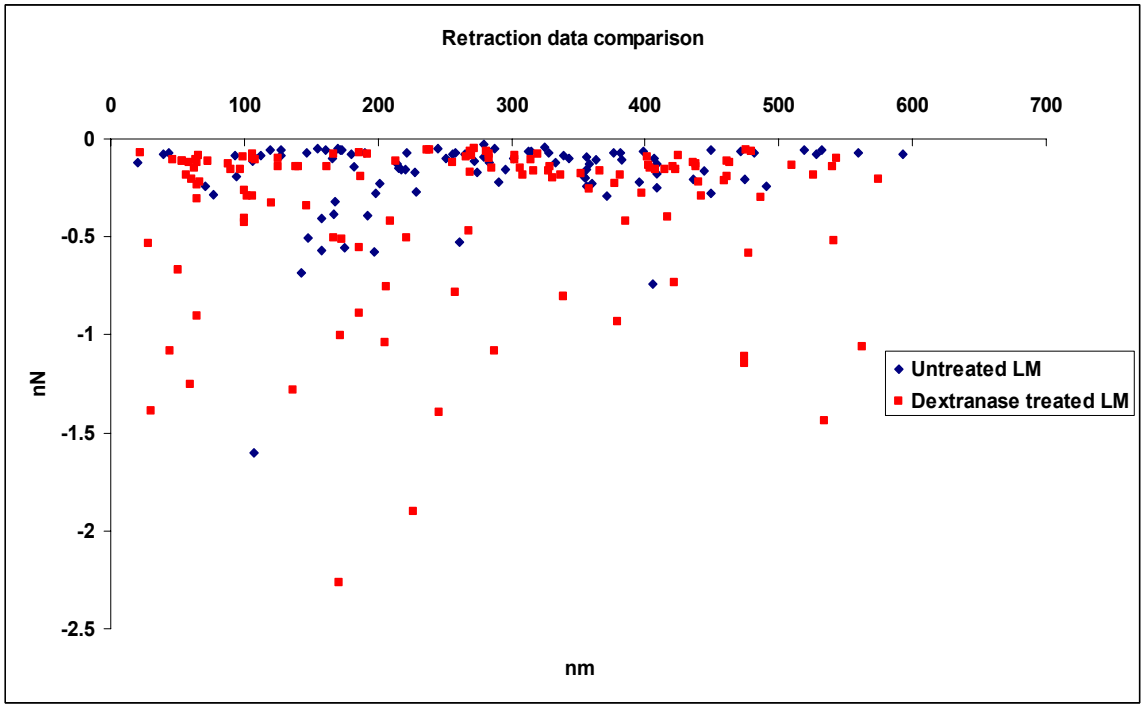

Figure 33: Comparison of retraction data between untreated and dextranase treated NIRC1542 cells

The results from the retraction curves of the untreated and dextranase treated NIRC1542 cells indicate increase in attractive forces after the cleavage of dextran from the cell surface. The results based on the retraction curves were compared on the basis of normalized number of instances of a certain magnitude of pull experienced by the AFM tip (**Figure 34**), and on the basis of the number of pull instances in a certain range of distance (**Figure 35**), for the dextranase treated and untreated cells.

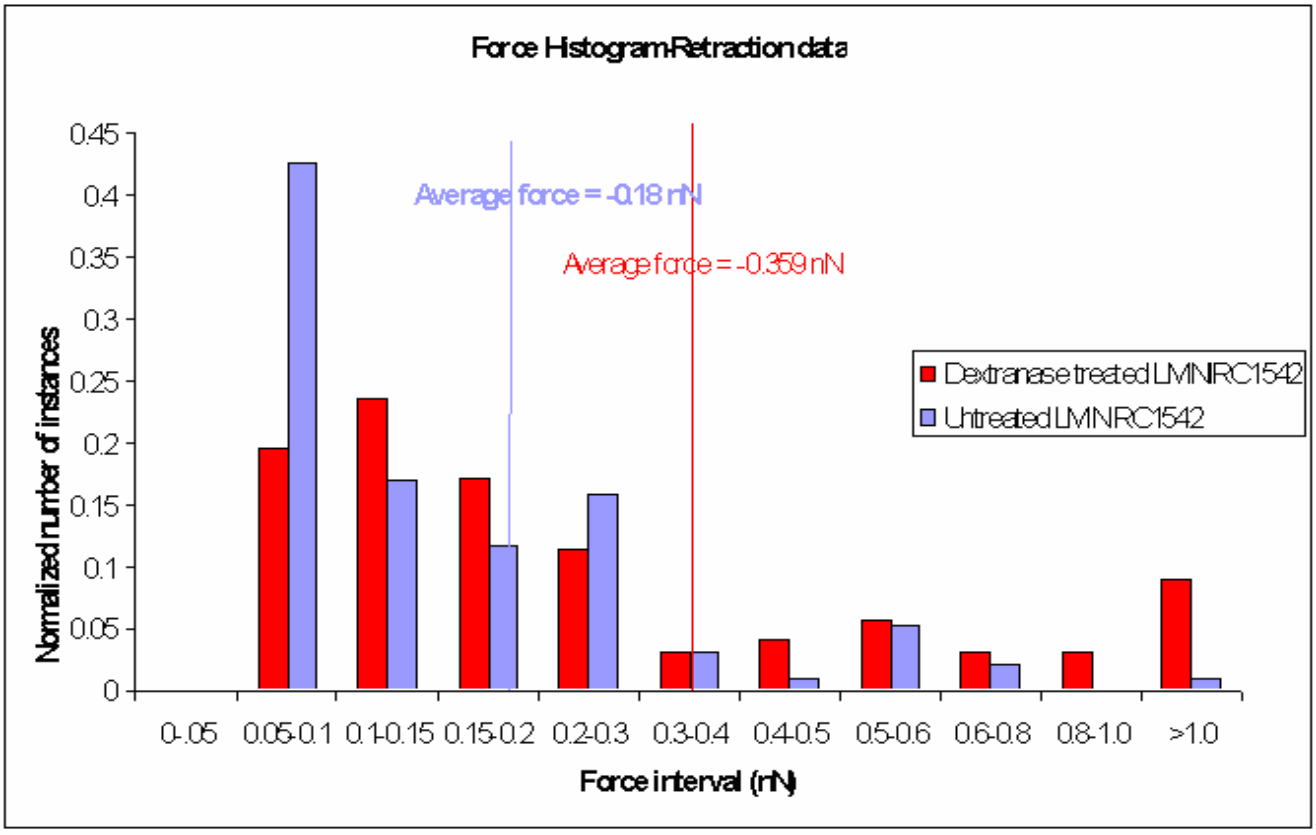

Figure 34: Comparison of normalized number of events occurring in a certain force range for each case

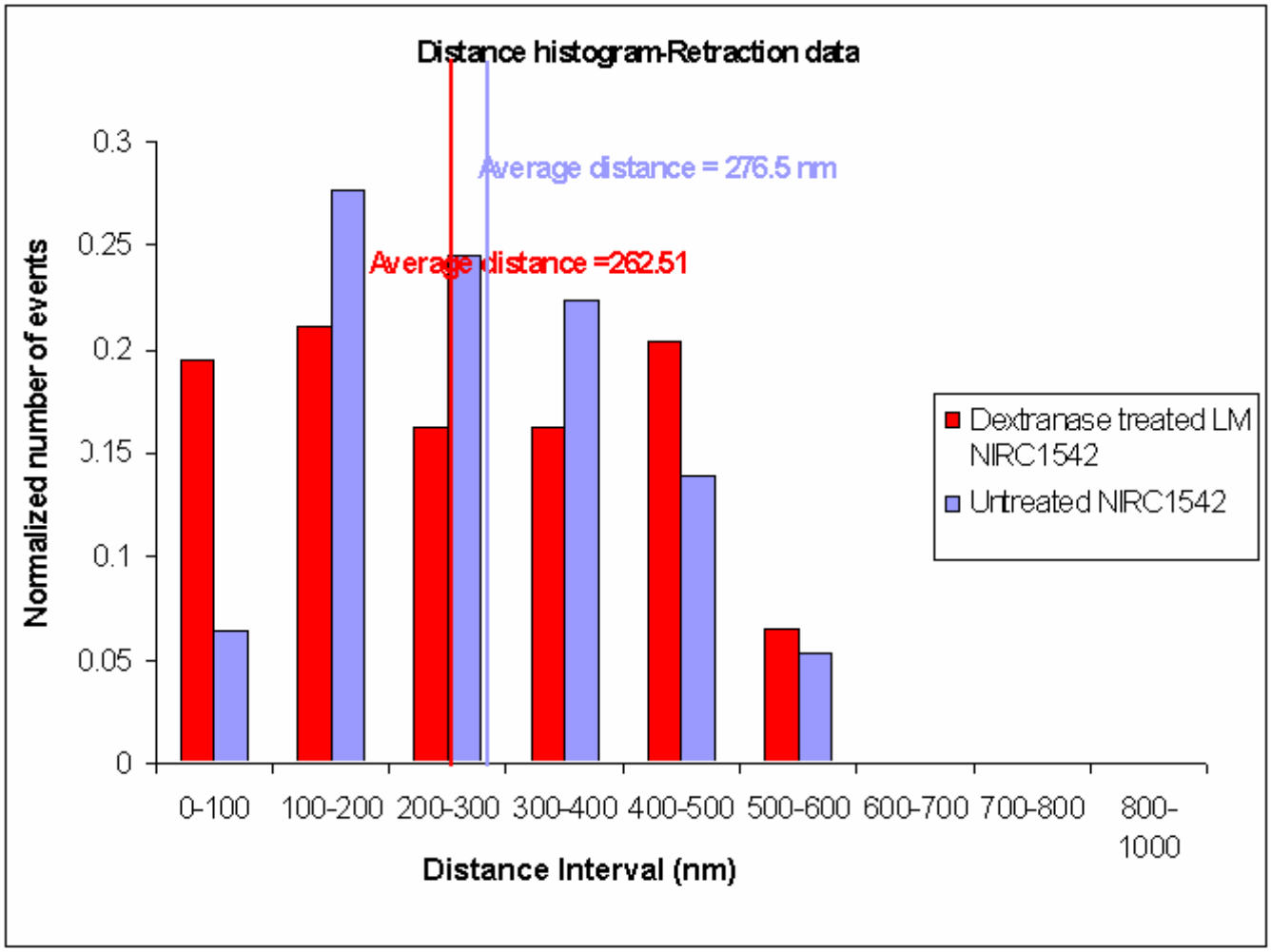

Figure 35: Comparison of normalized number of events occurring in a certain distance range for each case

Overall the force of repulsion decreased whereas the force of attraction increased after the enzyme treatment for the NIRC1542 cells with not much change in the length of the biopolymer chains present on the cell surface.

5.0 Conclusions

The results indicate the sensitivity of the atomic force microscopy in detecting the loss of polysaccharides from the surface of *Pseudomonas putida* KT2442 and *Leuconostoc mesenteroides* NIRC1542 bacteria upon their treatment with cellulase and dextranase, respectively.

The change in the behavior of force curves as detected with the help of AFM after treating KT2442 bacteria with cellulase indicates an appreciable amount of loss of cellulose from the surface of the cells which could be measured using AFM in terms of reduced repulsive force at the surface of the cell attributing to loss in density of the polysaccharides on the surface. Also the reduction in the range of force from the cell surface indicated shortening of the polymer brush on the cell surface after the enzyme treatment for *Pseudomonas putida* KT2442. Further analysis of the retraction curves for KT2442 shows reduced force of attraction due to the loss of cellulose from the surface indicating cellulose to be contributing towards adhesive nature of the cell.

Treating of the NIRC1542 cells with dextranase and studying them under AFM reveals reduced repulsive force at the surface after the treatment indicating loss in polymer brush density at the surface. The treatment with dextranase does not affect the polymer brush height on the cell surface as seen in results obtained from fitting approach curves to the steric model. Analysis of the retraction curves for enzyme treated NIRC1542 cells shows enhanced adhesion force suggesting the presence of dextran must be having a screening effect on other polymers with capacity of adhering to surfaces more strongly. As soon as the dextran is removed the cell surface and other polymers present on the surface show greater adhesive force.

Thus manipulating a bacterial cell for the polysaccharides present on its surface by treating it with a specific enzyme can make the bacterium more or less adhesive in nature. And AFM is a reliable instrument in understanding the effect of the specific enzyme on the bacterial cell surface properties.

References

Abu-Lail, N. I. and T. A. Camesano (2002). "Elasticity of Pseudomonas putida KT2442 surface polymers probed with single-molecule force microscopy." Langmuir **18**(10): 4071-4081.

Becker, K. and M. Wahl (1991). "Influence of substratum surface tensionon biofouling of artificial substratain Kiel Bay (Western Baltic): *In situ* studies." Biofouling **4**: 275.

Behrend, O. P., L. Odoni, J. L. Loubet and N. A. Burnham (1999). "Phase imaging: Deep or superficial?" Applied Physics Letters **75**(17): 2551-2553.

Boonaert, C. J. P. and P. G. Rouxhet (2000). "Surface of lactic acid bacteria: relationships between chemical composition and physicochemical properties." Applied and Environmental Microbiology **66**(6): 2548-2554.

Bowen, W. R., A. S. Fenton, R. W. Lovitt and C. J. Wright (2002). "The measurement of Bacillus mycoides spore adhesion using atomic force microscopy, simple counting methods, and a spinning disk technique." Biotechnology and Bioengineering **79**(2): 170-179.

Boyd, R. D., J. Verran, M. V. Jones and M. Bhakoo (2002). "Use of the atomic force microscope to determine the effect of substratum surface topography on bacterial adhesion." Langmuir **18**(6): 2343-2346.

Brant, D. A. (1999). "Novel approaches to the analysis of polysaccharide structures." Current Opinion in Structural Biology **9**(5): 556-562.

Bruinsma, G. M., M. Rustema-Abbing, J. de Vries, H. J. Busscher, M. L. van der Linden, J. M. M. Hooymans and H. C. van der Mei (2003). "Multiple surface properties of worn RGP lenses and adhesion of *Pseudomonas aeruginosa*." Biomaterials **24**(9): 1663-1670.

Buckwalter, M. S., C. M. Testa, J. L. Noebels and S. A. Camper (1993). "Genetic mapping and evaluation of candidate genes for spasmodic, a neurological mouse mutation with abnormal startle response." Genomics **17**(2): 279-86.

Burks, G. A. and S. B. Velegol (2003). "Macroscopic and nanoscale measurements of the adhesion of bacteria with varying outer layer surface composition." Langmuir **19**(6): 2366-2371.

Camesano, T. A. and B. E. Logan (1998). "Influence of Fluid Velocity and Cell Concentration on the Transport of Motile and Nonmotile Bacteria in Porous Media." Environmental Science and Technology **32**(11): 1699-1708.

Camesano, T. A. and B. E. Logan (2000). "Probing bacterial electrosteric interactions using atomic force microscopy." Environmental Science and Technology **34**(16): 3354-3362.

Camesano, T. A., K. M. Unice and B. E. Logan (1999). "Blocking and ripening of colloids in porous media and their implications for bacterial transport." Colloids and Surfaces, A: Physicochemical and Engineering Aspects **160**(3): 291-308.

Camesano, T. A. a. A.-L., Nehal I. (2002). "Heterogeneity in bacterial surface polysaccharides, probed on a single-molecule basis." Biomacromolecules **3**(4): 661-667.

Chao, K.-J., J. R. Kingsley, R. J. Plano, X. Lu and I. Ward (2001). "Applications of atomic force microscopy/scanning capacitance microscopy in imaging implant structures of semiconductor devices." Journal of Vacuum Science & Technology, B: Microelectronics and Nanometer Structures **19**(4): 1154-1157.

Clark, A. H. (1994). X-ray scattering and diffraction. Phys. Tech. Study Food Biopolym, Blackie, Glasgow, UK.

Cohen, Y. and E. Rosenberg (1989). Microbial Mats: Physiological Ecology of Benthic Microbial Communities. American Society for Microbiology, Washington, DC.

DeFlaun, M. F., S. R. Oppenheimer, S. Streger, C. W. Condee and M. Fletcher (1999). "Alterations in adhesion, transport, and membrane characteristics in an adhesion-deficient pseudomonad." Applied and Environmental Microbiology **65**(759): 759-765.

Dexter, S. C. (1979). "Influence of substratum critical surface tension on bacterial adhesion - in situ studies." Journal of Colloid and Interface Science **70**(2): 346-354.

Dumitriu, S. (1998). Polysaccharides: Structural Diversity and Functional Versatility.

Eberl, L., M. Givskov, L. Kongsbak Poulsen and S. Molin (1997). "Use of bioluminescence for monitoring the viability of individual Pseudomonas putida

KT2442 cells." FEMS Microbiology Letters **149**(1): 133-140.

Eberl, L., M. Givskov, C. Sternberg, S. Moeller, G. Christiansen and S. Molin (1996). "Physiological responses of Pseudomonas putida KT2442 to phosphate starvation." Microbiology **142**(1): 155-63.

Fasolka, M. J., A. M. Mayes and S. N. Magonov (2001). "Thermal enhancement of AFM phase contrast for imaging diblock copolymer thin film morphology." Ultramicroscopy **90**(1): 21-31.

Feldner, J., W. Bredt and I. Kahane (1983). "Influence of cell shape and surface charge on attachment of Mycoplasma pneumoniae to glass surfaces." Journal of Bacteriology **153**(1): 1-5.

Fisher, T. E., P. E. Marszalek, A. F. Oberhauser, M. Carrion-Vazquez and J. M. Fernandez (1999). "The micro-mechanics of single molecules studied with atomic force microscopy." Journal of Physiology **520**(1): 5-14.

Fletcher, M. and G. I. Loeb (1979). "Influence of substratum characteristics on the attachment of a marine Pseudomonad to solid surfaces." Applied and Envrionmental Microbiology **37**: 67-72.

Fletcher, M. and K. C. Marshall (1982). "Bubble contact angle method for evaluating substratum interfacial characteristics and its relevance to bacterial attachment." Applied and Environmental Microbiology **44**(1): 184-92.

Frank, B. P. and G. Belfort (1997). "Intermolecular Forces between Extracellular Polysaccharides Measured Using the Atomic Force Microscope." Langmuir **13**(23): 6234-6240.

Frank Caccavo, J. (1999). "Protein-Mediated Adhesion of the Dissimilatory Fe(III)-Reducing Bacterium Shewanella alga BrY to Hydrous Ferric Oxide." Applied And Environmental Microbiology **65**(11): 5017-22.

Gannon, J., Y. Tan, P. Baveye and M. Alexander (1991). "Effect of sodium chloride on transport of bacteria in a saturated aquifer material." Applied and Environmental Microbiology **57**(9): 2497-501.

Gannon, J. T., V. B. Manilal and M. Alexander (1991). "Relationship between cell surface properties and transport of bacteria through soil." Applied and Environmental Microbiology **57**: 190-193.

Grabar, K. C., R. G. Freeman, M. B. Hommer and M. J. Natan (1995).

"Preparation and Characterization of Au Colloid Monolayers." Analytical Chemistry **67**(4): 735-43.

Grabarek, Z. and J. Gergely (1990). "Zero-length crosslinking procedure with the use of active esters." Analytical Biochemistry **185**(1): 131-5.

Gu, X., M. VanLandingham, D. Raghavan and T. Nguyen (2000). "Mapping heterogeneity in polymeric materials using atomic force microscopy-phase imaging and nanoindentation." Polymeric Materials Science and Engineering **82**: 50-51.

Hermansson, A.-M. and M. Langton (1994). Electron microscopy, Blackie, Glasgow, UK.

Holmberg, K. and J. M. Harris (1995). Poly(ethylene glycol) grafting as a way to prevent protein adsorption and bacterial adherence. International Congress on Adhesion Science and Technology.

Israelachvili, J. N. (1992). Intermolecular & Surface Forces. NY.

Jhonson, C. R. and K. Mann (1986). "The crustose coralline alga, Phymatolithon foslie, inhebits the overgrowth of seaweeds without relying on herbivores." J Exp Mar Biol Ecol **96**: 127-146.

Keifer, P. A., K. L. Rinehart and I. R. Hooper (1986). "Renillafoulins, antifouling diterpenes from the sea pansy Renilla reniformis (Octocorallia)." Journal of Organic Chemistry **51**(23): 4450-4454.

Kowalewski, T. (1996). Atomic force microscopy of non-crystalline polymers - from nanoscale mechanical properties to surface topography. 212th ACS National Meeting, Orlando, FL, American Chemical Society.

Liu, C., X. Li, F. Xu and P. M. Huang (2003). "Atomic force microscopy of soil inorganic colloids." Soil Science and Plant Nutrition **49**(1): 17-23.

Ludwig, M., M. Rief, L. Schmidt, H. Li, F. Oesterhelt, M. Gautel and H. E. Gaub (1998). "AFM, a tool for single-molecule experiments." Materials Science & Processing **A68**(2): 173-176.

Macpherson, J. V., P. R. Unwin, A. C. Hillier and A. J. Bard (1996). "In-Situ Imaging of Ionic Crystal Dissolution Using an Integrated Electrochemical/AFM Probe." Journal of the American Chemical Society **118**(27): 6445-6452.

MacRae, I. C. and S. K. Evans (1983). "Factors influencing the adsorption of bacteria to magnetite in water and wastewater." Water Research **17**(3): 271-7.

Marszalek, P., H. Li and J. M. Fernandez (2001). "Fingerprinting polysaccharides with single-molecule atomic force microscopy." Nature Biotechnology **19**(3): 258-262.

Marszalek, P. E., Y.-P. Pang, H. Li, J. El Yazal, A. F. Oberhauser and J. M. Fernandez (1999). "Atomic levers control pyranose ring conformations." Proceedings of the National Academy of Sciences of the United States of America **96**(14): 7894-7898.

Mercer, J. R., R. M. Ford, J. L. Stitz and C. Bradbeer (1993). "Growth rate effects on fundamental transport properties of bacterial populations." Biotechnology and Bioengineering **42**(11): 1277-86.

Mittelman, M. W. (1998). "Structure and functional characteristics of bacterial biofilms in fluid processing operations." Journal of Dairy Science **81**(10): 2760-2764.

Ong, Y.-L., A. Razatos, G. Georgiou and M. M. Sharma (1999). "Adhesion Forces between E. coli Bacteria and Biomaterial Surfaces." Langmuir **15**(8): 2719-2725.

Ouwehand, A. C., T. Suomalainen, S. Tolkko and S. Salminen (2002). "In vitro adhesion of propionic acid bacteria to human intestinal mucus." Lait **82**(1): 123-130.

Park, S. B. (1999). "Characterization of inorganic particles by atomic force microscopy." Hwahak Konghak **37**(6): 904-909.

Paul, J. H. and G. I. Loeb (1983). "Improved microfouling assay employing a DNA-specific fluorochrome and polystyrene as substratum." Applied and Environmental Microbiology **46**(2): 338-43.

Pauli, A. T., W. Grimes, S. C. H. Huang and R. E. Robertson (2003). Surface energy studies of SHRP asphalts by AFM. 225th ACS National Meeting, New Orleans, LA, United States, American Chemical Society, Washington, D. C.

Poelstra, K. A., H. C. van der Mei, B. Gottenbos, D. W. Grainger, J. R. van Horn, H. J. Busscher and G. Anthony (2000). "Pooled human immunoglobulins reduce adhesion of Pseudomonas aeruginosa in a parallel plate flow chamber." Journal Of Biomedical Materials Research **51**(2): 224-32.

Poortinga, A. T., R. Bos and H. J. Busscher (2001). "Lack of effect of an externally applied electric field on bacterial adhesion to glass." Colloids and Surfaces, B: Biointerfaces **20**(2): 189-194.

Pringle, J. H. and M. Fletcher (1983). "Influence of substratum wettability on attachment of freshwater bacteria to solid surfaces." Applied and Environmental Microbiology **45**: 811-817.

Pringle, J. H. and M. Fletcher (1986). "The influence of substratum hydration and adsorbed macromolecules on bacterial attachment to surfaces." Applied and Environmental Microbiology **51**: 1321-1325.

Pringle, J. H., M. Fletcher and D. C. Ellwood (1983). "Selection of attachment mutants during the continuous culture of *Pseudomonas fluoroscens* and relationship between attachment ability and surface composition." Journal of General Microbiology **129**: 2557-2569.

Quinterto, E. J. and R. M. Weiner (1995). "Evidence for the adhesive function of the exopolysaccharide of *Hyphomonas* strain MHS-3 in its attachment to surfaces." Applied and Environmental Microbiology **61**: 1897-1903.

Raghavan, D., X. Gu, M. VanLandingham and T. Nguyen (2001). "Mapping chemically heterogeneous polymer system using selective chemical reaction and tapping mode atomic force microscopy." Macromolecular Symposia **167**: 297-305.

Ramphal, R., C. Guay and G. B. Pier (1987). "*Pseudomonas Aeruginosa* mucoid exopolysaccharide in adherence to tracheal cells." Infection and Immunity **55**: 600-603.

Ransom, B., R. H. Bennett, R. Baerwald and K. Shea (1997). "TEM study of in situ organic matter on continental margins: occurrence and the "Monolayer" hypothesis." Marine Geology **138**(1/2): 1-9.

Razatos, A., Y.-L. Ong, F. Boulay, D. L. Elbert, J. A. Hubbell, M. M. Sharma and G. Georgiou (2000). "Force Measurements between Bacteria and Poly(ethylene glycol)-Coated Surfaces." Langmuir **16**(24): 9155-9158.

Razatos, A., Y.-L. Ong, M. M. Sharma and G. Georgiou (1998). "Molecular determinants of bacterial adhesion monitored by atomic force microscopy." Proceedings of the National Academy of Sciences of the United States of America **95**(19): 11059-11064.

Rief, M., J. M. Fernandez and H. E. Gaub (1998). "Elastically Coupled Two-Level Systems as a Model for Biopolymer Extensibility." Physical Review Letters **81**(21): 4764-4767.

Rief, M., F. Oesterhelt, B. Heymann and H. E. Gaub (1997). "Single molecule force spectroscopy on polysaccharides by atomic force microscopy." Science **275**(5304): 1295-1297.

Rosowki, J. R. (1992). "Specificity of bacterial attachment sites on the filamentous diatom." Canadian Journal of Microbiology **38**: 676-686.

Round, A. N., M. Berry, T. J. McMaster, S. Stoll, D. Gowers, A. P. Corfield, M. J. Miles and H. H. Wills (2002). "Heterogeneity and persistence length in human ocular mucins." Biophysical Journal **83**(3): 1661-1670.

Rouxhet, P. G. and M. J. Genet (1991). "Chemical composition of the microbial cell surface by x-ray photoelectron spectroscopy." Microbiology and Cell Surface Analysis: 173-220.

Samanta, S. K. and R. K. Jain (2000). "Evidence for plasmid-mediated chemotaxis of Pseudomonas putida towards naphthalene and salicylate." Canadian Journal of Microbiology **46**(1): 1-6.

Scott, M. H. and L. C. Gregory (1998). "Differentiation of Dextran-Producing Leuconostoc Strains by a Modified Randomly Amplified Polymorphic DNA protocol." Applied and Environmental Microbiology **64**(8): 3096-3098.

Seaman, J. C., P. M. Bertsch and W. P. Miller (1995). "Chemical Controls on Colloid Generation and Transport in a Sandy Aquifer." Environmental Science and Technology **29**(7): 1808-15.

Sharma, M. M., Y. I. Chang and T. F. Yen (1985). "Reversible and irreversible surface charge modification of bacteria for facilitating transport through porous media." Colloids and Surfaces **16**(2): 193-206.

Shellenberger, K. and B. E. Logan (2002). "Effect of molecular scale roughness of glass beads on colloidal and bacterial deposition." Environmental Science & Technology **36**(2): 184-9.

Shilo, M. (1989). The unique characteristics of benthic cyanobacteria. American Society for Microbiology, Washington, DC.

Simoni, S. F., H. Harms, T. N. P. Bosma and A. J. B. Zhender (1998). "Population Heterogeneity Affects Transport of Bacteria through Sand Columns at Low Flow Rates." Environmental Science and Technolgy **32**(2100): 2100-2105.

Singjai, P., N. Songmee, T. Tunkasiri and T. Vilaithong (2002). "Atomic force microscopy imaging and cutting of beaded carbon nanotubes deposited on glass." Surface and Interface Analysis **33**(10/11): 900-904.

Sorongon, M. L., R. A. Bloodgood and R. P. Burchard (1991). "Hydrophobicity, adhesion, and surface-exposed proteins of gliding bacteria." Applied and Environmental Microbiology **57**(11): 3193-9.

Staros, J. V., R. W. Wright and D. M. Swingle (1986). "Enhancement by N-hydroxysulfosuccinimide of water-soluble carbodiimide-mediated coupling reactions." Analytical Biochemistry **156**(1): 220-2.

Stenstrom, T. A. (1998). "Bacterial hydrophobicity, an overall parameter for the measurement of adhesion potential to soil particles." Applied and Environmental Microbiology **55**(1): 142-7.

Sturgeon, R. J. (1983). "General methods." Carbohydrate Chemistry **14**(2): 5-20.

Sutherland, I. W. (1998). "Novel and established applications of microbial polysaccharides." Trends in Biotechnolgy **16**(1): 41-6.

Todd, J. S., R. C. Zimmerman, P. Crews and S. A. Randall (1993). "The antifouling activity of natural and synthetic phenolic acid sulfate esters." Phytochemistry **34**: 401-404.

Tombs, M. and S. Harding (1997). An Introduction to Polysaccharide Biotechnology. Nottingham.

Triandafillu, K., D. J. Balazs, B.-O. Aronsson, P. Descouts, P. Tu Quoc, C. van Delden, H. J. Mathieu and H. Harms (2003). "Adhesion of *Pseudomonas aeruginosa* strains to untreated and oxygen-plasma treated poly(vinyl chloride) (PVC) from endotracheal intubation devices." Biomaterials **24**(1507): 1507-18.

Vadillo-Rodriguez, V., H. J. Busscher, W. Norde, J. de Vries and H. C. van der Mei (2003). "On Relations between Microscopic and Macroscopic Physicochemical Properties of Bacterial Cell Surfaces: An AFM Study on Streptococcus mitis Strains." Langmuir **19**(6): 2372-2377.

Van der Mei, H. C., P. Brokke, J. Dankert, J. Feijen, P. G. Rouxhet and H. J. Busscher (1989). "Physicochemical surface properties of nonencapsulated and encapsulated coagulase-negative staphylococci." Applied and Environmental Microbiology **55**(11): 2806-14.

Van Pelt, A. W. J., A. H. Weerkamp, M. Uyen, H. J. Busscher, H. P. De Jong and J. Arends (1985). "Adhesion of Streptococcus sanguis CH3 to polymers with different surface free energies." Applied and Environmental Microbiology **49**(5): 1270-5.

Velegol, S. B. and B. E. Logan (2002). "Contributions of bacterial surface polymers, electrostatics, and cell elasticity to the shape of AFM force curves." Langmuir **18**(13): 5256-5262.

Vignon, M. R. and C. Garcia-Jaldon (1996). "Structural features of the pectic polysaccharides isolated from retted hemp bast fibers." Carbohydrate Research **296**: 249-260.

Villetti, M., R. Borsali, O. Diat, V. Soldi and K. Fukada (2000). "SAXS from polyelectrolyte solutions under shear: xanthan and sodium-hyaluronate examples." Macromolecules **33**(25): 9418-9422.

Weiss, T. H., A. L. Mills, G. M. Hornberger and J. S. Herman (1995). "Effect of Bacterial Cell Shape on Transport of Bacteria in Porous Media." Environmental Science and Technology **29**(7): 1737-40.

Williams, V. and M. Fletcher (1996). "Pseudomonas fluorescens adhesion and transport through porous media are affected by lipopolysaccharide composition." Applied and Environmental Microbiology **62**(100): 100-104.

Yao, X., J. Walter, S. Burke, S. Stewart, M. H. Jericho, D. Pink, R. Hunter and T. J. Beveridge (2002). "Atomic force microscopy and theoretical considerations of surface properties and turgor pressures of bacteria." Colloids and Surfaces, B: Biointerfaces **23**(2-3): 213-230.